



Thinning of articular cartilage after joint unloading or immobilization. An experimental investigation of the pathogenesis in mice

Nomura, Masato ; Sakitani, Naoyoshi ; Iwasawa, Hiroyuki ; Kohara, Yuta ; Takano, Shoko ; Wakimoto, Yoshio ; Kuroki, Hiroshi ; Moriyama, Hideki

(Citation)

Osteoarthritis and Cartilage, 25(5):727-736

(Issue Date)

2017-05

(Resource Type)

journal article

(Version)

Accepted Manuscript

(Rights)

© 2016 Osteoarthritis Research Society International. Published by Elsevier. This manuscript version is made available under the CC-BY-NC-ND 4.0 license <http://creativecommons.org/licenses/by-nc-nd/4.0/>

(URL)

<https://hdl.handle.net/20.500.14094/90004510>



1 **Thinning of articular cartilage after joint unloading or immobilization. An experimental**
2 **investigation of the pathogenesis in mice**

3

4 Masato Nomura, M.Sc., Naoyoshi Sakitani, M.Sc., Hiroyuki Iwasawa, M.Sc., Yuta Kohara,

5 B.Sc., Shoko Takano, B.Sc., Yoshio Wakimoto, M.Sc., Hiroshi Kuroki, Ph.D., Hideki

6 Moriyama, Ph.D.

7

8 M. Nomura (cunorimousiraty@gmail.com)

9 N. Sakitani (7asdfghjklzxcvbnm@gmail.com)

10 Y. Kohara (kohakoha1313@gmail.com)

11 S. Takano (shoko.12.t@gmail.com)

12 Y. Wakimoto (wakio0820.kbu@gmail.com)

13 H. Moriyama (morihide@harbor.kobe-u.ac.jp)

14 Department of Rehabilitation Science, Graduate School of Health Sciences, Kobe University.,

15 Tomogaoka 7-10-2, Suma-ku, Kobe 654-0142, Japan.

16

17 H. Iwasawa (googrie588@gmail.com)

18 Department of Rehabilitation, St. Marianna University School of Medicine., Sugao 2-16-1,

19 Miyamae-ku, Kawasaki 216-8511, Japan

20 Department of Rehabilitation Science, Graduate School of Health Sciences, Kobe University.,

21 Tomogaoka 7-10-2, Suma-ku, Kobe 654-0142, Japan.

22

23 H. Kuroki (kuroki.hiroshi.6s@kyoto-u.ac.jp)

24 School of Health Sciences, Graduate School of Medicine, Kyoto University., Kawahara-cho,

25 Shogoin 53, Sakyo-ku, Kyoto-shi, Kyoto 606-8507, Japan.

26

27 Corresponding author:

28 Hideki Moriyama, Ph.D.

29 Professor

30 Department of Rehabilitation Science, Graduate School of Health Sciences, Kobe University

31 Tomogaoka 7-10-2, Suma-ku, Kobe 654-0142, Japan.

32 Tel & Fax +81 78 796 4574

33 E-mail morihide@harbor.kobe-u.ac.jp

34

35 Running title: Cartilage degeneration by disuse

36 **Abstract**

37 *Objective:* Moderate mechanical stress generated by normal joint loading and movement is
38 essential for the maintenance of healthy articular cartilage. However, the effects of reduced
39 loading caused by the absence of weight bearing or joint motion on articular cartilage and
40 subchondral bone is still poorly understood. We aimed to characterize morphological and
41 metabolic responses of articular cartilage and subchondral bone to decreased mechanical
42 stress in vivo.

43 *Methods:* Mice were subjected to periods of hindlimb unloading by tail suspension or
44 external fixation of the knee joints. The articular surface was observed with digital
45 microscope and the epiphyseal bone was assessed by micro-CT analysis. Articular cartilage
46 and subchondral bone were further evaluated by histomorphometric, histochemical, and
47 immunohistochemical analyses.

48 *Results:* The joint surface was intact, but thickness of both the total and uncalcified layer of
49 articular cartilage were decreased both after joint unloading and immobilization. Subchondral
50 bone atrophy with concomitant marrow expansion predisposed osteoclast activity at bone
51 surface to invade into cartilaginous layer. Uncalcified cartilage showed decreased aggrecan
52 content and increased aggrecanase expression. Alkaline phosphatase activity was increased at
53 uncalcified cartilage, whereas decreased at calcified cartilage. The distributions of
54 hypertrophic chondrocyte markers remained unchanged.

55 *Conclusion:* Thinning of articular cartilage induced by mechanical unloading may be
56 mediated by metabolic changes in chondrocytes, including accelerated aggrecan catabolism
57 and exquisitely modulated matrix mineralization, and cartilage matrix degradation and
58 resorption by subchondral osteoclasts. Cartilage degeneration without chondrocyte
59 hypertrophy under unloading condition indicate the possible existence of mechanism which is
60 different from osteoarthritis pathogenesis.

61

62 *Key words:* Mechanical unloading, Articular cartilage, Aggrecan, Mineralization,
63 Subchondral bone, Osteoclast

64 **Introduction**

65

66 Moderate mechanical stress generated by normal joint loading and movement is
67 essential for the maintenance of healthy articular cartilage. Although cartilage within a
68 physiological range of mechanical stress assures the optimal balance between anabolic and
69 catabolic phenomena¹, overloading induces catabolic chondrocyte responses² and is well
70 known to be one of the main causes of osteoarthritis (OA)³. In addition, the reduction of
71 applied load (caused by joint disuse) has also been reported to be harmful to articular
72 cartilage⁴.

73

74 Animal models of joint unloading or immobilization have been used extensively to
75 study the effects of decreased mechanical stress on joint structures, including articular
76 cartilage. Numerous animal studies demonstrated that joint immobilization by casting or
77 surgery induces changes in cartilage thickness⁵⁻¹⁵, number of chondrocytes⁸⁻¹⁷, extracellular
78 matrix components^{7,9-25}, and cartilage surface irregularity or fibrillation^{11-17,25-27}. These
79 alterations were often associated with contracture development. However, most of these
80 animal studies on joint immobilization observed articular cartilage mainly at the contact areas
81 in fixed position, and several authors including Langenskiöld *et al.*²⁵ attributed this cartilage
82 degradation by loss of joint motion to compression necrosis, rather than reduced loading.

83 Only 5 prior studies attempted to assess the influence of joint unloading without motion
84 restriction on the articular cartilage, using animal models of ipsilateral paw transection²⁹ or
85 tail suspension^{5,30-32}. In these studies, unloading led to increased or decreased or unchanged
86 thickness of cartilage^{5,29,31,32}, decreased or unchanged number of chondrocytes^{29,30,32},
87 existence or non-existence of chondrocyte hypertrophy and cluster^{29,31,32}, reduced
88 proteoglycan content^{29,31,32}, tidemark advancement^{5,31}, and existence or non-existence of
89 subchondral vascular encroachment into the cartilage^{5,31}.

90

91 There has been a growing interest in the effect of reduced loading on articular
92 cartilage, since a recent study on patients with ankle fracture reported that 7 weeks of partial
93 load bearing led to decrease in knee cartilage thickness, volume, and surface area³³. However,
94 in earlier animal studies^{5,29-32}, there is no consensus about morphological changes of articular
95 cartilage after unloading. In addition, chondrocyte differentiation, survival, and metabolic
96 characteristics in the pathogenesis is still poorly investigated, and cross-talk between
97 subchondral bone and articular cartilage under unloading condition remains unclear. Despite
98 the clinical importance of cartilage degeneration by disuse such as during prolonged bed rest
99 or long-term space flight, exercise is the only effective safeguard conceivable, as its
100 pathology remain elusive.

101

102 The goal of this study was to gain a comprehensive picture of pathology in cartilage
103 alteration by mechanical unloading. We applied hindlimb unloading by tail suspension or
104 surgical immobilization of the knee joints in mice. Entire knee joints are exposed to
105 unloading in tail suspended mice, while non-contact regions in immobilized mice. We
106 examined morphological responses of articular cartilage and subchondral bone after
107 mechanical unloading, and sought to determine possible pathological factors contributing to
108 the morphological changes.

109

110 **Method**

111

112 *Experimental animals and animal care*

113

114 Thirty male C57BL/6J mice of 7 weeks of age were purchased from Japan SLC
115 (Shizuoka, Japan). Acclimated for 1 week, randomly selected six mice were killed and served
116 as control, while the remaining 24 mice were equally divided into two experimental groups:
117 hindlimb unloaded (HU) and immobilized (IM). The animals in each experimental group
118 were assigned to 3 subgroups (n = 4 per group), corresponding to the time of examination
119 after unweighting or immobilization: 2, 4, and 8 weeks.

120

121 For the HU group, animals underwent tail suspension with a modified unloading
122 method based on the traditional NASA Morey-Holton design³⁴. Briefly, mice were
123 anesthetized by intraperitoneal administration of 40 mg/kg sodium pentobarbital and
124 subcutaneously injected with 0.02 mg/kg buprenorphine to give relief of pain. A sterile steel
125 wire was inserted into an intervertebral space of the tail and the steel wire was shaped into a
126 ring for later suspension. Connecting the tail ring by string to track hanged from the ceiling,
127 we enabled the animals to roam freely throughout the entire cage. The head down tilt angle
128 was monitored every day throughout the experimental period and remained at approximately
129 30° [Supplementary Fig. 1(A)], so that 50% of the body weight was distributed to the
130 forelimbs³⁵.

131

132 The right and left knees of each animal in the IM group were surgically immobilized
133 according to the modified method described by Nagai *et al.*³⁶. In brief, a longitudinal incision
134 was made through the lateral skin of the femur and the tibia under anesthesia. 2 cm-long
135 kirschner wires of 0.6 mm in diameter were then screwed into the both diaphyses. After the
136 skin were closed with silk suture, the two kirschner wires were externally fixed with wire and
137 resin to maintain knee flexion of approximately $140 \pm 5^\circ$ [Supplementary Fig. 1(B)].
138 Postoperatively, the animals had appropriate pain control by subcutaneous dose of 0.02
139 mg/kg buprenorphine once daily for 5 days. We confirmed in a pilot study that kirschner

140 wires penetrated through bones and no fracture occurred by micro-computed tomography
141 (μ CT) scanning [Supplementary Fig. 1(C)] and that rigid immobilization was maintained for
142 more than 8 weeks after surgery.

143

144 The right and left knees served as different samples. They were housed in plastic
145 cages in a room with controlled environmental conditions, and had free access to water and
146 standard food. This study was approved by the Institutional Animal Care and Use Committee
147 and carried out according to the Kobe University Animal Experimentation Regulation.

148

149 *Microscopic and Scanning Electron Microscopic (SEM) Observation*

150

151 At the end of the experimental period, the half of the animals in each group were
152 euthanized by exsanguination under anesthesia. Knee joints were removed by dissection and
153 disarticulated. Entire articular surface of the femoral condyle and tibial plateau were imaged
154 using digital microscope (VHX-5000; Keyence, Osaka, Japan) and high-resolution zoom lens
155 (VH-ZST; Keyence) under x 200 magnification. SEM images were subsequently obtained at
156 the magnification of x 2000 with free-angle observation system (VHX-D510; Keyence).

157

158 *μ CT Analysis*

159

160 After the observations of cartilage surface, the samples of distal femur and proximal
161 tibia were scanned separately by micro 3D x-ray CT system (R_mCT2; Rigaku, Tokyo,
162 Japan) with an isotropic voxel resolution of 10 μm (x-ray tube potential = 90 kV, current =
163 160 μA , and a scan time of 3 min per sample). 3D images were reconstructed and were
164 analyzed with TRI/3D-BON software (Ratoc, Tokyo, Japan). Bone volume density (bone
165 volume/total volume; BV/TV) were measured on the epiphyseal regions.

166

167 *Histology*

168

169 *Histological preparation*

170

171 Undecalcified frozen sections were prepared according to the method described by
172 Kawamoto³⁷. Briefly, the whole knee joints including the patella and joint capsule were
173 harvested from the animals of half the number in each group. Knee samples were then freeze-
174 embedded with 5% carboxymethyl cellulose gel at the angle of maximum flexion
175 (approximately $140 \pm 5^\circ$; equal to that of immobilized). Blocks were cut into slices from
176 medial side of the knees, and 5- μm sagittal sections were prepared at the level which is 50-
177 200 μm lateral from the level that the medial meniscus separates into anterior and posterior

178 horns.

179

180 *Determination of Regions for Assessment*

181

182 We originally determined the cartilage regions for assessment in the medial
183 femorotibial joint according to their positions in embedded joints (Fig. 1). The posterior
184 femur (FP) and posterior tibia (TP) were defined as the regions of articular cartilage located
185 between the inner edges of the anterior and posterior meniscal horns. The edges of the
186 anterior femoral (FA) and anterior tibial (TA) regions were located beyond the outer edges of
187 the anterior meniscal horn. The middle femoral (FM) and middle tibial (TM) cartilage were
188 situated between the FA and FP regions or between the TA and TP regions, and located
189 adjacent to the anterior horn of the meniscus. In our pilot study, FM and TM regions
190 contacted each other when the joint bent at 80° flexion [Supplementary Fig. 1(D)], which is
191 the approximate flexion observed at the beginning of the gait in small rodents and when
192 maximum contact pressure is expected in the load-bearing regions of the joint³⁸. Results for
193 histological assessments of articular cartilage were also expressed as the mean values of these
194 six regions.

195

196 *Histomorphometric analysis*

197

198 According to the modification of our previous method³⁹, articular cartilage thickness
199 was measured on digitized images of histological sections stained with toluidine blue, which
200 provides excellent color discrimination between bone and calcified cartilage, as well as a
201 distinct basophilic line that marks the location of the tidemark⁵. Briefly, at each region, a 200
202 μm -long stretch of the cartilage surface was defined and the areas of the uncalcified and
203 calcified cartilage under this stretch were measured separately. The thickness of each layer
204 was calculated by dividing the area by 200 μm . Total cartilage thickness was the sum of the
205 thickness of uncalcified and calcified layer. The mean thickness for each specimen was
206 derived by averaging measurements from three slides spaced 50 μm apart.

207

208 Chondrocyte density was measured on the sections stained with Weigert's iron
209 hematoxylin. The cartilage area was measured using the same method as cartilage thickness,
210 and cells with visible nuclei in the area were counted manually. Chondrocyte density was
211 determined as the number of chondrocytes per cartilage area.

212

213 *Histochemical Analysis*

214

215 Alkaline phosphatase (ALP) and tartrate-resistant acid phosphatase (TRAP) activity

216 were detected according to the manufacturers' instructions (Sigma, St. Louis, MO, USA), and
217 these sections were counterstained with eosin or Alcian blue, respectively. ALP-positive
218 chondrocytes were counted manually at each cartilage region. TRAP-stained histological
219 images were split into separate channels, and TRAP-positive cells at the entire epiphysis were
220 identified on the red channel grayscale images by a certain threshold, using Image J 1.50
221 (National Institutes of Health, Bethesda, MD, USA). The TRAP-positive area per total area
222 was calculated. In addition, osteoclast surface reaching articular cartilage was traced
223 manually and the length was measured. The values were normalized by the length of
224 osteochondral junction.

225

226 *Immunohistochemical Analysis*

227

228 Following the protocols established in our laboratory⁴⁰, sections were
229 immunostained using antibody against type II collagen (diluted 1:150, ab21291; Abcam,
230 Tokyo, Japan), aggrecan (diluted 1:400, AB1031; Millipore, Billerica, MA, USA), matrix
231 metalloproteinase 13 (MMP13; diluted 1:100, AB8120; Millipore), a disintegrin and
232 metalloproteinase with thrombospondin motifs 5 (ADAMTS5; diluted 1:75, ab41037;
233 Abcam), type X collagen (diluted 1:1000, LB-0092; LSL, Tokyo, Japan), vascular endothelial
234 growth factor (VEGF; diluted 1:400, ABS82; Millipore), receptor activator of nuclear factor

235 kappa-B ligand (RANKL; diluted 1:100, sc-7628; Santa Cruz, Dallas, TX, USA), and
236 osteoprotegerin (OPG; diluted 1:100, ab73400; Abcam). Immunoreactivity was visualized
237 with 3,3'-diaminobenzidine tetrahydrochloride (K3466; Dako Japan, Tokyo, Japan). On
238 undecalcified frozen sections prepared using Kawamoto's film method, hematoxylin stains
239 calcified tissues³⁷. Therefore we used hematoxylin as counter staining in order to distinguish
240 calcified region (deep zone of articular cartilage where calcified cartilage occupies more) and
241 uncalcified region.

242

243 For type II collagen and aggrecan, histological images were converted to grayscale
244 images with Adobe Photoshop CS2 (Adobe Systems, San Jose, CA, USA). The mean of pixel
245 gray values (in the range 0 to 255) was measured with image J. Staining intensity was
246 calculated by the following formula: Staining intensity = 255 – mean gray value

247

248 For MMP13, ADAMTS5, type X collagen, VEGF, RANKL, and OPG, the number
249 of immune-positive cells was manually counted. Dividing the number of RANKL-positive
250 cells by the number of OPG-positive cells, RANKL/OPG ratio was calculated.

251

252 *Statistical Analysis*

253

254 Statistical analyses were conducted with SPSS (IBM developer Works, Japan. IBM
255 SPSS statistical 23). First, all data were checked for normality with the Shapiro-Wilk test.
256 When normality was observed in all assays, the results were compared among all groups with
257 the ANOVA test followed by the Tukey HSD test. All values are presented here as mean \pm
258 standard deviation (SD). *P* values less than 0.05 were considered significant.

259

260 **Result**

261

262 *Microstructure of Articular Surface*

263

264 The articular cartilage of femoral condyle and tibial plateau in both the experimental
265 groups were intact macroscopically [Supplementary Fig. 2(A)]. The appearance of the
266 cartilage surface by SEM also showed no differences among the groups [Supplementary Fig.
267 2(B)].

268

269 *Cartilage Thickness and chondrocyte density*

270

271 Cartilage matrix staining to toluidine blue, which reflect proteoglycan content, was
272 decreased at uncalcified cartilage at posterior regions in the HU group and anterior regions in

273 the IM group [Fig. 2(A)]. Mean cartilage thickness of the six regions are shown in Fig. 2(B).
274 Uncalcified cartilage of the HU group (2 weeks, $43.9 \pm 2.0 \mu\text{m}$; 4 weeks, $40.8 \pm 1.1 \mu\text{m}$; 8
275 weeks, $37.9 \pm 2.2 \mu\text{m}$) and the IM group (2 weeks, $43.1 \pm 2.5 \mu\text{m}$; 4 weeks, $40.0 \pm 1.0 \mu\text{m}$; 8
276 weeks, $35.7 \pm 3.1 \mu\text{m}$) were significantly decrease at all time points, when compared to the
277 control group ($49.9 \pm 2.5 \mu\text{m}$, $P < 0.01$). Moreover, thickness in total layer of articular
278 cartilage were significantly decreased at 8 weeks in the HU group ($97.2 \pm 2.7 \mu\text{m}$) and at 4
279 and 8 weeks in the IM group (4 weeks, $100.6 \pm 4.8 \mu\text{m}$; 8 weeks, $93.8 \pm 8.2 \mu\text{m}$), when
280 compared with the control group ($116.5 \pm 4.0 \mu\text{m}$, $P < 0.01$). Notably, the thickness in total
281 and uncalcified layer at TP region in the IM group were not different from the control group
282 at any time points (Supplementary Table 1).

283

284 Chondrocyte density in the HU group was comparable to that in the control group
285 and normal appearance of the nuclei was observed [Fig. 2(C and D)]. In the IM group, on the
286 other hand, significantly less cellularity was detected at all time points (versus control, $P <$
287 0.01). The group showed chondrocytic lacunae with picnotic or absent nuclei at FA, FM, TA,
288 and TM region and decreased intensity of nuclear staining at FP and TP regions. Cell clusters
289 were not found.

290

291 *Cartilage Matrix and Proteases*

292

293 As disclosed by immunohistochemistry, type II collagen was evenly distributed
294 throughout the cartilage [Fig. 3(A)], and the staining intensity showed no differences among
295 the groups [Fig. 3(B)]. The expression of MMP13, which is the most active in cleaving type
296 II collagen, were barely detectable in chondrocytes at calcified layer [Fig. 3(A)]. Although
297 the number of MMP13-positive cells showed no differences among the groups [Fig. 3(B)],
298 immunoreactivity for MMP13 was also present at the bone surface corresponding to the
299 lower edges of articular cartilage in both the experimental groups.

300

301 The control cartilage showed strong immunostaining for aggrecan, the major
302 proteoglycan in cartilage, uniformly across the entire cartilage [Fig. 3(C)]. The experimental
303 groups exhibited significantly less staining at uncalcified cartilage at 2 weeks (versus control,
304 $P < 0.01$) [Fig. 3(D)]. ADAMTS5, the major aggrecanase in mouse cartilage, was distributed
305 within chondrocytes in the control group, whereas both secreted and nuclear-localized
306 cellular ADAMTS5 were detected in the experimental groups [Fig. 3(C)]. ADAMTS5-
307 positive cells at uncalcified cartilage were increased at all time points in the HU group and 2
308 weeks in the IM group (versus control, $P < 0.05$) [Fig. 3(D)].

309

310 *ALP activity and Hypertrophic Chondrocyte Markers*

311

312 ALP activity, which is involved in regulating mineralization of cartilage and bone⁴¹,
313 was located in chondrocytes on tidemark and at calcified cartilage in the control group [Fig. 4
314 (A)]. The number of ALP-positive cells were not changed at total layer. However, the number
315 showed significant increase at uncalcified layer and decrease at calcified layer in the
316 experimental groups (versus control, $P < 0.05$) [Fig. 4(B)].

317

318 The expression of type X collagen, specific marker of chondrocyte hypertrophy, was
319 observed only at cells in calcified cartilage in all groups [Fig. 4(A)]. The number of type X
320 collagen-positive cells was not different among the groups [Fig. 4(B)]. Similarly, VEGF,
321 which is synthesized by hypertrophic chondrocytes, were strongly expressed in chondrocytes
322 at calcified layer [Fig. 4(A)]. The number of VEGF-positive cells was decreased at total and
323 uncalcified layer in the experimental groups (versus control, $P < 0.05$), but showed no
324 differences at calcified layer among the groups [Fig. 4(B)].

325

326 *Bone Structure and osteoclast activity*

327

328 On μ CT images, Trabecular bone was appeared to be decreased at the entire
329 epiphysis in the HU group, while the bone loss was evident at the anterior area in the IM

330 group [Fig. 5(A)]. BV/TV were significantly decreased in the HU group (2 weeks, $45.9 \pm$
331 5.3% ; 4 weeks, $52.6 \pm 2.9\%$; 8 weeks, $47.2 \pm 1.3\%$) and the IM group (2 weeks, $40.4 \pm 7.7\%$;
332 4 weeks, $41.6 \pm 1.6\%$; 8 weeks, $46.6 \pm 8.5\%$) when compared to the control group ($59.9 \pm$
333 3.1% ; $P < 0.05$) [Fig. 5(B)].

334

335 Histological images of the epiphysis showed similar findings of bone atrophy and
336 expanded subchondral bone marrow space reached the articular cartilage [Fig. 5 (C)]. TRAP
337 staining as an indicator of osteoclastic activity revealed that increased bone resorption
338 occurred at entire epiphysis [Fig. 5(D)]. Subchondral bone loss with concomitant marrow
339 expansion predisposed osteoclast activity at bone surface to invade into articular cartilage.
340 Percentage of TRAP-positive area in the epiphyseal region and osteoclast surface reaching
341 articular cartilage were markedly increased at 2 weeks in both the experimental groups when
342 compared to the control group ($P < 0.05$) [Fig. 5(E and F)].

343

344 Immunohistochemistry revealed protein expressions of RANKL and OPG at
345 articular chondrocytes [Supplementary Fig. 3(A)]. The number of RANKL-positive
346 chondrocytes were increased in the HU group (versus control, $P < 0.05$) [Supplementary Fig.
347 3(B)]. Furthermore, both the experimental groups showed significant decrease in the number
348 of OPG-positive chondrocytes at calcified layer (versus control, $P < 0.05$). RANKL/OPG

349 ratio at calcified layer increased 3.5-fold in the HU group and 3.1-fold in the IM group.

350

351 **Discussion**

352

353 This study demonstrated that reduced loading by the absence of weight bearing or
354 external fixation led to decreased thickness of both the total and uncalcified layer of articular
355 cartilage. The aggrecan content was decreased and ADAMTS5 expression was increased at
356 uncalcified cartilage after joint unloading or immobilization, but unloading did not alter the
357 chondrocyte density, distribution, and morphology, indicating the loss of aggrecan results
358 from altered chondrocyte metabolism rather than apoptosis. No changes in the distributions
359 of type X collagen imply that the cartilage thinning and matrix loss by mechanical unloading
360 may not be mediated by hypertrophic differentiation of chondrocytes. TRAP activity
361 penetrating into the articular cartilage associated with subchondral bone atrophy represents
362 cartilage resorption by osteoclasts and may contribute to the cartilage thinning. Increased
363 RANKL/OPG ratio in articular chondrocytes may be partly responsible for the subchondral
364 osteoclast activation. Reduced ALP activity at calcified cartilage suggest suppressed
365 mineralization at the layer and may promote further expansion of subchondral marrow. Our
366 findings of no fibrillation at the articular surface support the notion that the cartilage
367 alterations observed in this study is not due to overloading or shear stress, but results from

368 decreased mechanical stress.

369

370 After hindlimb unloading, uncalcified layer of articular cartilage was thinned at 2
371 weeks, whereas total layer at 8 weeks. These results indicate that 4 or less weeks of
372 experimental period are too short to detect changes in total thickness of articular cartilage
373 following joint unloading, which may explain the discordances among the results in earlier
374 studies^{5,30-32}. TP region, which was the dominant weight bearing area in tibia of the fixed
375 knee joint [Supplementary Fig. 1(D)], showed no changes in cartilage thickness throughout
376 the experiment after joint immobilization. This finding supports the Carter's theory that
377 cyclic hydrostatic forces generated through joint loading maintain articular cartilage
378 thickness⁴².

379

380 Some animal studies of joint unloading have reported reduction in safranin O or
381 toluidine blue staining at articular cartilage^{29,31,32}, indicating the loss of proteoglycans. Our
382 results suggest that mechanical unloading elicits aggrecan degradation through increased
383 expression of ADAMTS5. Uncoupling of systemic type II collagen synthesis and degradation
384 after hindlimb unloading has been reported, where serum pCol-II-C and urinary CTx-II levels
385 were analyzed³¹. Although these biomarkers have been developed to evaluate turnover of
386 type II collagen, they have low specificity. In this study, we directly analyzed the

387 distributions of type II collagen in the knee articular cartilage after joint unloading or
388 immobilization and confirmed that no changes occurred. Our results imply that the loss of
389 proteoglycans is more severe than or precede collagen alterations under unloading condition.

390

391 In OA pathogenesis, upregulation of matrix-degrading enzymes following
392 chondrocyte hypertrophy contributes to cartilage destruction⁴³. We observed increased
393 expression of ADAMTS5 and loss of aggrecan at uncalcified cartilage. Nevertheless, the
394 distributions of hypertrophic chondrocyte markers remained unchanged. These results
395 indicate the possible existence of mechanism not via chondrocyte hypertrophy by which
396 reduced load induces matrix degradation. Chondrocyte apoptosis, which increases in
397 osteoarthritic cartilage⁴³, contributes to the risk of articular cartilage degeneration via its role
398 in extracellular matrix production and maintenance. Morphological changes of articular
399 chondrocytes have been commonly reported to be observed after joint immobilization⁸⁻¹⁷,
400 whereas not after joint unloading without motion restriction²⁹. Our results are congruent with
401 these reports. However, a recent study³⁰ demonstrated that 2 weeks of hindlimb unloading
402 resulted in a marked increase in apoptotic chondrocytes and inducible nitric oxide synthase-
403 positive chondrocytes in rats. Further investigations are warranted to determine whether
404 reduced mechanical loading affect chondrocyte survival.

405

406 It is well accepted that disuse bone atrophy arises from increase in bone resorption
407 and/or decrease in bone formation⁴⁴. Both joint unloading and immobilization showed a
408 significant decrease in bone volume density and a marked increase in TRAP activity at entire
409 epiphysis including subchondral bone in this study. RANKL and OPG, which are known to
410 be key molecules in the regulation of osteoclast activity, are generally produced by
411 osteoblasts/stromal cells, as well as chondrocytes⁴⁵. Increase in RANKL/OPG ratio at
412 calcified cartilage after joint unloading or immobilization may partly contribute to osteoclast
413 activation at subchondral bone. Mature osteoclasts have shown to be capable of expression of
414 MMPs⁴⁶ and cartilage matrix resorption⁴⁷. We found MMP13 activity distributed at the bone
415 surface corresponding to the lower edge of articular cartilage and TRAP activity invasion into
416 articular cartilage, which may represent matrix degradation and resorption by osteoclasts.
417 These findings support the concept that thinning of articular cartilage by mechanical
418 unloading is the result of osteoclastic cartilage resorption. ALP activity is required for
419 preparation of mineralization⁴⁸, and generally localized to hypertrophic cells in cartilage⁴⁹, as
420 shown in the control mice of this study. Decrease in ALP-positive cells at calcified cartilage
421 in the experimental groups represent decline in constant mineral apposition at the layer,
422 which may allow subchondral marrow expansion extend to cartilaginous layer through a
423 relative increase in bone resorption.

424

425 O'Connor⁵, who observed mineral apposition rate at the tidemark after hindlimb
426 unloading in rats, have attributed thinning of uncalcified cartilage by unweighting to
427 advancement of tidemark mineralization front toward the joint surface. Subsequently, Tomiya
428 *et al.*³¹ proposed that the tidemark advancement stem largely from loss of proteoglycans,
429 which inhibit mineralization, and that increase in ALP activity would be necessary to cause
430 the advancement. Our findings of decreased proteoglycan content and increased ALP activity
431 at uncalcified layer support this hypothesis of Tomiya *et al.*³¹. ALP activity is thought to
432 localized to hypertrophic cells in cartilage⁴⁸. Nevertheless, the distributions of ALP activity
433 did not correspond with those of hypertrophic chondrocyte markers in the experimental
434 groups. We showed here that chondrocytes can present ALP activity without hypertrophic
435 differentiation and ALP activity is not necessarily localized to hypertrophic chondrocytes.
436 However, how mechanical unloading modulates ALP activity in chondrocytes warrants future
437 examination.

438

439 A major limitation of the present study was that the effects of aging cannot be ruled
440 out since we had no age-matched controls. Although it is well known that aging leads to
441 cartilage degeneration⁴⁰, thickness of articular cartilage and structure of epiphyseal
442 cancellous bone has reported to be not altered with aging in young C57BL/6 mice at least up
443 to 16-weeks-old⁵⁰. We therefore regarded 8-weeks-old mice with no intervention as control of

444 all experimental groups, and this approach has the advantages of minimizing the number of
445 animals. Hindlimbs of immobilized animals exhibited slight signs of inflammation such as
446 edema for a few days postsurgery. The secretion of inflammatory cytokines or
447 neuroendocrine response induced by operative stress may affect the knee articular cartilage or
448 subchondral bone. However, it has been shown that sham surgery (wire insertion without
449 external fixation) did not elicit cartilage degeneration^{15,16}.

450

451 In conclusion, we propose that mechanical unloading induces thinning of articular
452 cartilage via acceleration of aggrecan catabolism, modulation of cartilage matrix
453 mineralization, and subchondral osteoclast activation (Fig. 6). Reduced loading did not affect
454 specific markers for chondrocyte hypertrophy and therefore may induces cartilage
455 degeneration in a different manner than overloading, suggesting that the vast body of
456 knowledge already gained from studies on OA cannot be fully applied to cartilage
457 degeneration by disuse.

458

459 **Acknowledgements**

460

461 We would like to acknowledge Dr. Momoko Nagai for advises on the surgical
462 immobilization. We also acknowledge the skillful technical assistance of Mr. Kosuke

463 Watanabe and Mr. Tomohiro Yoshikawa.

464

465 **Author contributions**

466

467 Conception and design of the study: MN, NS, HI, HK, and HM.

468 Analysis and interpretation of the data: MN, NS, HI, YK, YW, and HM.

469 Drafting of the article: MN.

470 Critical revision of the article for important intellectual content: HM.

471 Final approval of the article: all co-authors.

472 Statistical expertise: MN, YK, and HM.

473 Obtaining of funding: HM.

474 Collection and assembly of data: MN, NS, HI, YK, and ST.

475

476 **Role of the funding source**

477

478 This study was supported in part by Japan Society for the Promotion of Science

479 (JSPS) KAKENHI Grant Number 25702032.

480

481 **Competing interest statement**

482

483

The authors have no conflicts of interest to disclose.

484 **References**

485

486 1. Madry H, Luyten FP, Facchini A. Biological aspects of early osteoarthritis. *Knee Surg*
487 *Sports Traumatol Arthrosc* 2012;20:407-22.

488 2. Bleuel J, Zaucke F, Brüggemann GP, Niehoff A. Effects of cyclic tensile strain on
489 chondrocyte metabolism: a systematic review. *PLoS One* 2015;10:e0119816.

490 3. Silverwood V, Blagojevic-Bucknall M, Jinks C, Jordan JL, Protheroe J, Jordan KP.
491 Current evidence on risk factors for knee osteoarthritis in older adults: a systematic
492 review and meta-analysis. *Osteoarthritis Cartilage* 2015;23:507-15.

493 4. Vanwanseele B, Lucchinetti E, Stüssi E. The effects of immobilization on the
494 characteristics of articular cartilage: current concepts and future directions. *Osteoarthritis*
495 *Cartilage* 2002;10:408-19.

496 5. O'Connor KM. Unweighting accelerates tidemark advancement in articular cartilage at
497 the knee joint of rats. *J Bone Miner Res* 1997;12:580-9.

498 6. Iqbal K, Khan Y, Minhas LA. Effects of immobilization on thickness of superficial zone
499 of articular cartilage of patella in rats. *Indian J Orthop* 2012;46:391-4.

500 7. Kiviranta I, Jurvelin J, Tammi M, Säämänen AM, Helminen HJ. Weight bearing controls
501 glycosaminoglycan concentration and articular cartilage thickness in the knee joints of
502 young beagle dogs. *Arthritis Rheum* 1987;30:801-9.

- 503 8. Maldonado DC, Silva MC, Neto Sel-R, de Souza MR, de Souza RR. The effects of joint
504 immobilization on articular cartilage of the knee in previously exercised rats. *J Anat*
505 2013;222:518-25.
- 506 9. Sood SC. A study of the effects of experimental immobilisation on rabbit articular
507 cartilage. *J Anat* 1971;108:497-507.
- 508 10. Palmoski M, Perricone E, Brandt KD. Development and reversal of a proteoglycan
509 aggregation defect in normal canine knee cartilage after immobilization. *Arthritis Rheum*
510 1979;22:508-17.
- 511 11. Paukkonen K, Jurvelin J, Helminen HJ. Effects of immobilization on the articular
512 cartilage in young rabbits. A quantitative light microscopic stereological study. *Clin*
513 *Orthop Relat Res* 1986;206:270-80.
- 514 12. Trudel G, Himori K, Uthoff HK. Contrasting alterations of apposed and unapposed
515 articular cartilage during joint contracture formation. *Arch Phys Med Rehabil*
516 2005;86:90-7.
- 517 13. Ando A, Hagiwara Y, Chimoto E, Hatori K, Onoda Y, Itoi E. Intra-articular injection of
518 hyaluronan diminishes loss of chondrocytes in a rat immobilized-knee model. *Tohoku J*
519 *Exp Med* 2008;215:321-31.
- 520 14. Hagiwara Y, Ando A, Chimoto E, Saijo Y, Ohmori-Matsuda K, Itoi E. Changes of
521 articular cartilage after immobilization in a rat knee contracture model. *J Orthop Res*

- 522 2009;27:236-42.
- 523 15. Nagai M, Ito A, Tajino J, Iijima H, Yamaguchi S, Zhang X, *et al.* Remobilization causes
524 site-specific cyst formation in immobilization-induced knee cartilage degeneration in an
525 immobilized rat model. *J Anat* 2016;228:929-39.
- 526 16. Nagai M, Aoyama T, Ito A, Tajino J, Iijima H, Yamaguchi S, *et al.* Alteration of cartilage
527 surface collagen fibers differs locally after immobilization of knee joints in rats. *J Anat*
528 2015;226:447-57.
- 529 17. Thaxter TH, Mann RA, Anderson CE. Degeneration of immobilized knee joints in rats;
530 histological and autoradiographic study. *J Bone Joint Surg Am* 1965;47:567-85.
- 531 18. Behrens F, Kraft EL, Oegema TR Jr. Biochemical changes in articular cartilage after joint
532 immobilization by casting or external fixation. *J Orthop Res* 1989;7:335-43.
- 533 19. Jortikka MO, Inkinen RI, Tammi MI, Parkkinen JJ, Haapala J, Kiviranta I, *et al.*
534 Immobilisation causes longlasting matrix changes both in the immobilised and
535 contralateral joint cartilage. *Ann Rheum Dis* 1997;56:255-61.
- 536 20. Slowman SD, Brandt KD. Composition and glycosaminoglycan metabolism of articular
537 cartilage from habitually loaded and habitually unloaded sites. *Arthritis Rheum*
538 1986;29:88-94.
- 539 21. Säämänen AM, Tammi M, Jurvelin J, Kiviranta I, Helminen HJ. Proteoglycan alterations
540 following immobilization and remobilization in the articular cartilage of young canine

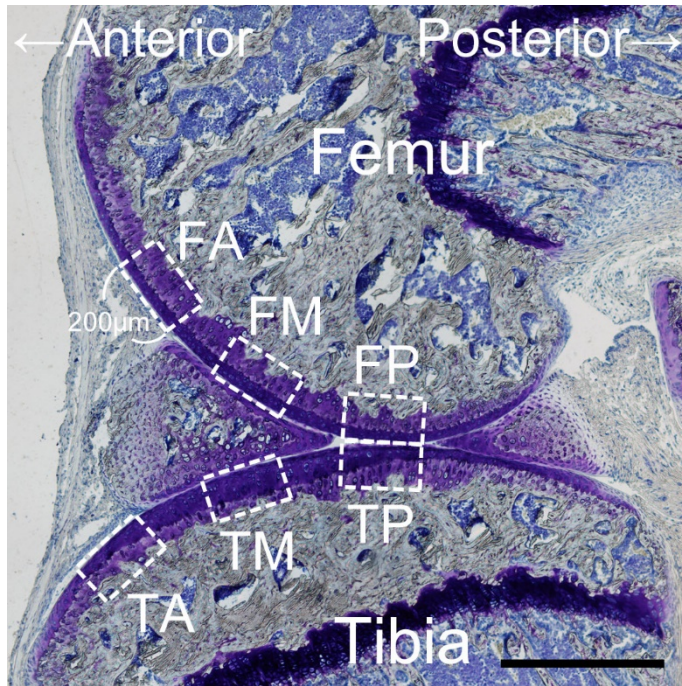
- 541 knee (stifle) joint. J Orthop Res 1990;8:863-73.
- 542 22. Videman T, Eronen I, Friman C. Glycosaminoglycan metabolism in experimental
543 osteoarthritis caused by immobilization. The effects of different periods of
544 immobilization and follow-up. Acta Orthop Scand 1981;52:11-21.
- 545 23. Videman T, Eronen I, Candolin T. [3H]proline incorporation and hydroxyproline
546 concentration in articular cartilage during the development of osteoarthritis caused by
547 immobilization. A study in vivo with rabbits. Biochem J 1981;200:435-40.
- 548 24. Hagiwara Y, Ando A, Chimoto E, Tsuchiya M, Takahashi I, Sasano Y, *et al.* Expression
549 of collagen types I and II on articular cartilage in a rat knee contracture model. Connect
550 Tissue Res 2010;51:22-30.
- 551 25. Langenskiöld A, Michelsson JE, Videman T. Osteoarthritis of the knee in the rabbit
552 produced by immobilization. Attempts to achieve a reproducible model for studies on
553 pathogenesis and therapy. Acta Orthop Scand 1979;50:1-14.
- 554 26. Józsa L, Järvinen M, Kannus P, Réffy A. Fine structural changes in the articular cartilage
555 of the rat's knee following short-term immobilisation in various positions: a scanning
556 electron microscopical study. Int Orthop 1987;11:129-33.
- 557 27. Jurvelin J, Helminen HJ, Lauritsalo S, Kiviranta I, Säämänen AM, Paukkonen K, *et al.*
558 Influences of joint immobilization and running exercise on articular cartilage surfaces of
559 young rabbits. A semiquantitative stereomicroscopic and scanning electron microscopic

- 560 study. *Acta Anat (Basel)* 1985;122:62-8.
- 561 28. Ando A, Hagiwara Y, Tsuchiya M, Onoda Y, Suda H, Chimoto E, *et al.* Increased
562 expression of metalloproteinase-8 and -13 on articular cartilage in a rat immobilized knee
563 model. *Tohoku J Exp Med* 2009;217:271-8.
- 564 29. Palmoski MJ, Colyer RA, Brandt KD. Joint motion in the absence of normal loading
565 does not maintain normal articular cartilage. *Arthritis Rheum* 1980;23:325-34.
- 566 30. Basso N, Heersche JN. Effects of hind limb unloading and reloading on nitric oxide
567 synthase expression and apoptosis of osteocytes and chondrocytes. *Bone* 2006;39:807-
568 14.
- 569 31. Tomiya M, Fujikawa K, Ichimura S, Kikuchi T, Yoshihara Y, Nemoto K. Skeletal
570 unloading induces a full-thickness patellar cartilage defect with increase of urinary
571 collagen II CTx degradation marker in growing rats. *Bone* 2009;44:295-305.
- 572 32. Luan HQ, Sun LW, Huang YF, Wu XT, Niu H, Liu H, *et al.* Use of micro-computed
573 tomography to evaluate the effects of exercise on preventing the degeneration of articular
574 cartilage in tail-suspended rats. *Life Sci Space Res (Amst)* 2015;6:15-20.
- 575 33. Hinterwimmer S, Krammer M, Krötz M, Glaser C, Baumgart R, Reiser M, *et al.*
576 Cartilage atrophy in the knees of patients after seven weeks of partial load bearing.
577 *Arthritis Rheum* 2004;50:2516-20.
- 578 34. Ferreira JA, Crissey JM, Brown M. An alternant method to the traditional NASA

- 579 hindlimb unloading model in mice. *J Vis Exp* 2011;49:2467.
- 580 35. Hargens AR, Steskal J, Johansson C, Tipton CM. Tissue fluid shift, forelimb loading, and
581 tail tension in tail-suspended rats. *Physiologist* 1984;27:37-8.
- 582 36. Nagai M, Aoyama T, Ito A, Iijima H, Yamaguchi S, Tajino J, *et al.* Contributions of
583 biarticular myogenic components to the limitation of the range of motion after
584 immobilization of rat knee joint. *BMC Musculoskelet Disord* 2014;15:224.
- 585 37. Kawamoto T, Kawamoto K. Preparation of thin frozen sections from nonfixed and
586 undecalcified hard tissues using Kawamoto's film method (2012). *Methods Mol Biol*
587 2014;1130:149-64.
- 588 38. Das Neves Borges P, Forte AE, Vincent TL, Dini D, Marenzana M. Rapid, automated
589 imaging of mouse articular cartilage by microCT for early detection of osteoarthritis and
590 finite element modelling of joint mechanics. *Osteoarthritis Cartilage* 2014;22:1419-28.
- 591 39. Moriyama H, Yoshimura O, Kawamata S, Takayanagi K, Kurose T, Kubota A, *et al.*
592 Alteration in articular cartilage of rat knee joints after spinal cord injury. *Osteoarthritis*
593 *Cartilage* 2008;16:392-8.
- 594 40. Moriyama H, Kanemura N, Brouns I, Pintelon I, Adriaensen D, Timmermans JP, *et al.*
595 Effects of aging and exercise training on the histological and mechanical properties of
596 articular structures in knee joints of male rat. *Biogerontology* 2012;13:369-81.
- 597 41. Bellows CG, Heersche JN, Aubin JE. Inorganic phosphate added exogenously or

- 598 released from beta-glycerophosphate initiates mineralization of osteoid nodules in vitro.
599 Bone Miner 1992;17:15-29.
- 600 42. Carter DR, Wong M. The role of mechanical loading histories in the development of
601 diarthrodial joints. J Orthop Res 1988;6:804-16.
- 602 43. Husa M, Liu-Bryan R, Terkeltaub R. Shifting HIFs in osteoarthritis. Nat Med
603 2010;16:641-4.
- 604 44. Dehority W, Halloran BP, Bikle DD, Curren T, Kostenuik PJ, Wronski TJ, *et al.* Bone
605 and hormonal changes induced by skeletal unloading in the mature male rat. Am J
606 Physiol 1999;276:62-9.
- 607 45. Funck-Brentano T, Cohen-Solal M. Crosstalk between cartilage and bone: when bone
608 cytokines matter. Cytokine Growth Factor Rev. 2011;22:91-7.
- 609 46. Andersen TL, del Carmen Ovejero M, Kirkegaard T, Lenhard T, Foged NT, Delaissé JM.
610 A scrutiny of matrix metalloproteinases in osteoclasts: evidence for heterogeneity and for
611 the presence of MMPs synthesized by other cells. Bone 2004;35:1107-19.
- 612 47. Knowles HJ, Moskovsky L, Thompson MS, Grunhen J, Cheng X, Kashima TG, *et al.*
613 Chondroclasts are mature osteoclasts which are capable of cartilage matrix resorption.
614 Virchows Arch 2012;461:205-10.
- 615 48. Roach HI. Association of matrix acid and alkaline phosphatases with mineralization of
616 cartilage and endochondral bone. Histochem J 1999;31:53-61.

- 617 49. Miao D, Scutt A. Histochemical localization of alkaline phosphatase activity in
618 decalcified bone and cartilage. *J Histochem Cytochem* 2002;50:333-40.
- 619 **50.** Ko FC, Dragomir C, Plumb DA, Goldring SR, Wright TM, Goldring MB, *et al.* In vivo
620 cyclic compression causes cartilage degeneration and subchondral bone changes in
621 mouse tibiae. *Arthritis Rheum* 2013;65:1569-78.



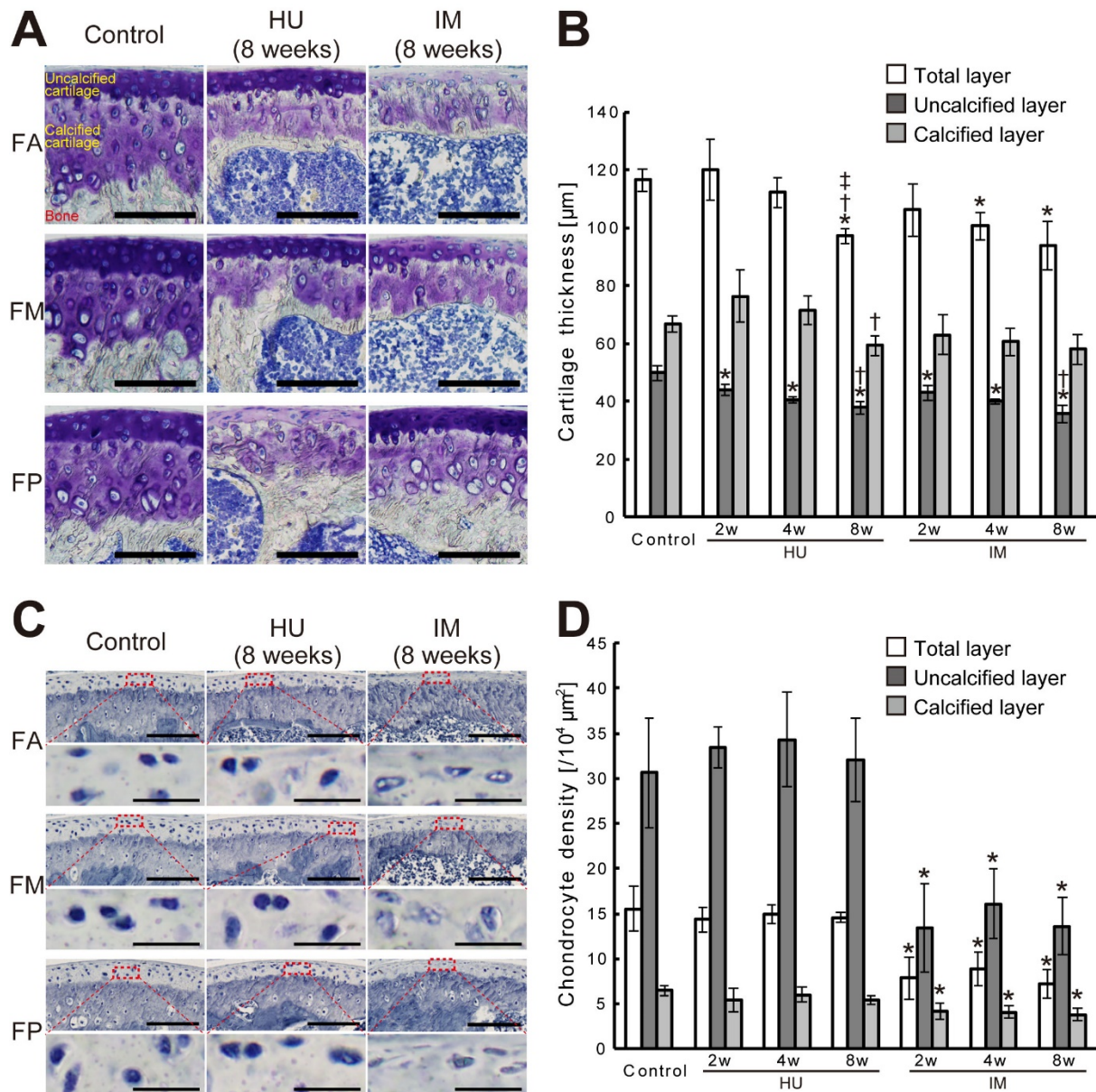
622

623 **Fig. 1.** Knee cartilage regions for histological evaluation were determined on sagittal section

624 at the medial midcondylar level. Assessment was performed at each region of 200 μm in

625 width. Toluidine blue staining. Scale bar = 500 μm. Cartilage region: FA, FM, FP, TA, TM,

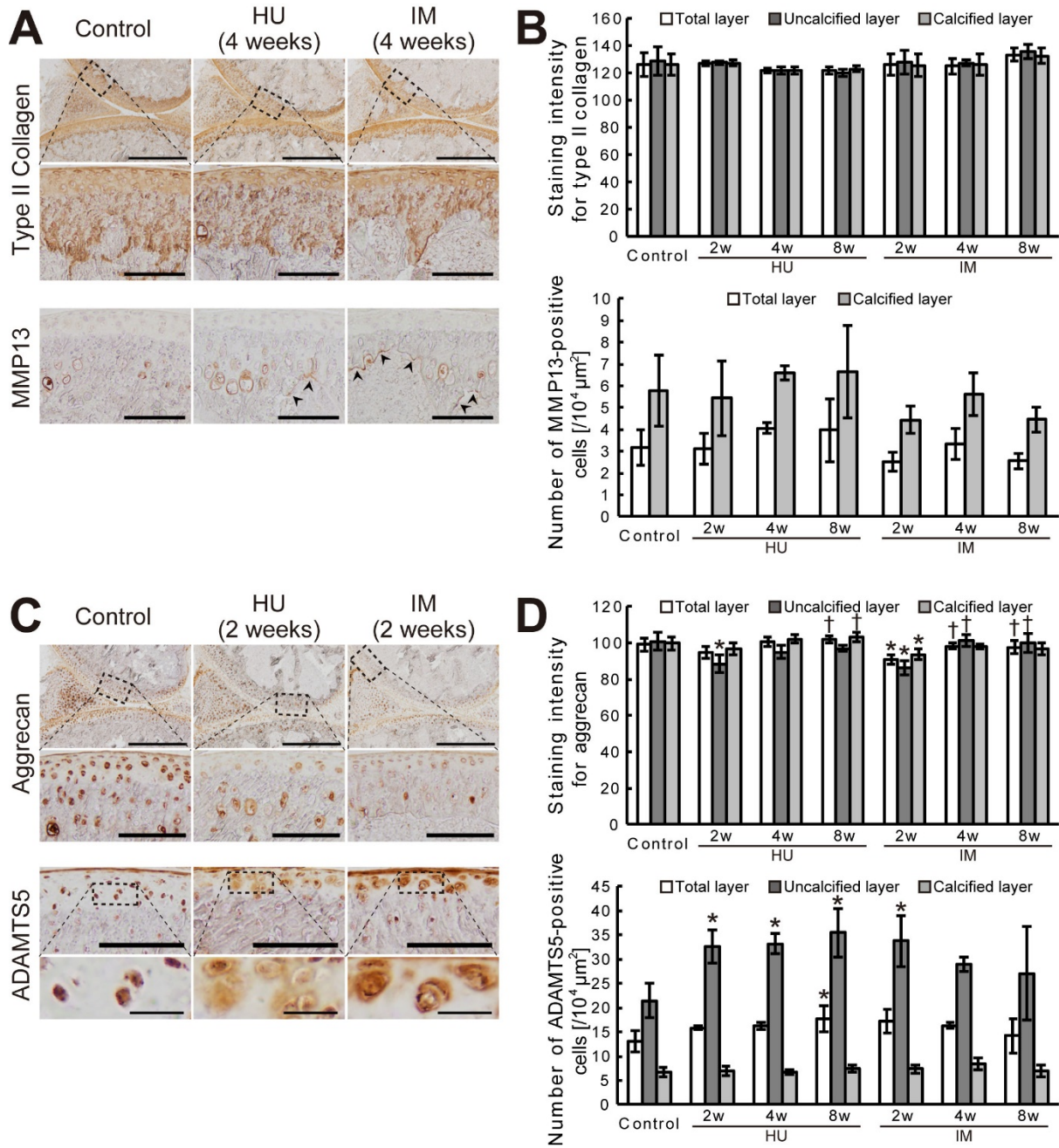
626 and TP.



627

628 **Fig. 2.** Cartilage thickness and chondrocyte density. (A) Thickness in uncalcified and
 629 calcified layer of articular cartilage were measured separately on the histological sections
 630 stained with toluidine blue. Staining intensity was decreased at uncalcified layer in FP region
 631 of the HU group and FA regions of the IM group. Scale bars = 100 μm . (B) Mean cartilage
 632 thickness of the six regions. At 8 weeks, both of the experimental groups showed significant
 633 decrease in thickness of total and uncalcified layer. Results for each region are shown in

634 Supplementary Table 1. (C) Histological observations of chondrocyte density (upper row;
635 scale bars = 100 μm) and morphology (lower row, scale bars = 20 μm). Chondrocytes in the
636 IM group showed picnotic nuclei, lacunae without nuclei, and less intensity of nuclear
637 staining. Weigert's iron hematoxylin staining. (D) Mean chondrocyte density of the six
638 regions. Only the IM group showed significantly less density. Results for each region are
639 shown in Supplementary Table 2. * Significant differences from the control group. †
640 Significant differences from the 2 weeks after the same intervention. ‡ Significant differences
641 from the 4 weeks after the same intervention. Cartilage region: FA, FM, FP.



642

643 **Fig. 3.** Distributions of cartilage matrixes and expressions of matrix proteases. (A)

644 Immunostaining for type II collagen was seen strongly in articular cartilage at all regions in

645 all groups. MMP13 expression was observed in chondrocyte at calcified layer. In the HU and

646 IM groups, immunolabeling was also detected at bone surface corresponding with the lower

647 edges of articular cartilage in the HU and IM groups (arrow head). Scale bars = 500 μm

648 (upper row of type II collagen), 100 μm (lower row of type II collagen and MMP13). (B)

649 Staining intensity for type II collagen and the number of MMP13-positive cells. Mean values

650 of the six regions. Results for each region are shown in Supplementary Table 3 and 4. (C)

651 Aggrecan was distributed throughout the whole cartilage. Higher-magnification views of the

652 boxed areas show less intensity at uncalcified layer in the HU and IM groups. ADAMTS5

653 was barely detectable in chondrocytes in the control, whereas the pericellular regions of

654 uncalcified cartilage were clearly stained in the HU and IM groups. Scale bars = 500 μm

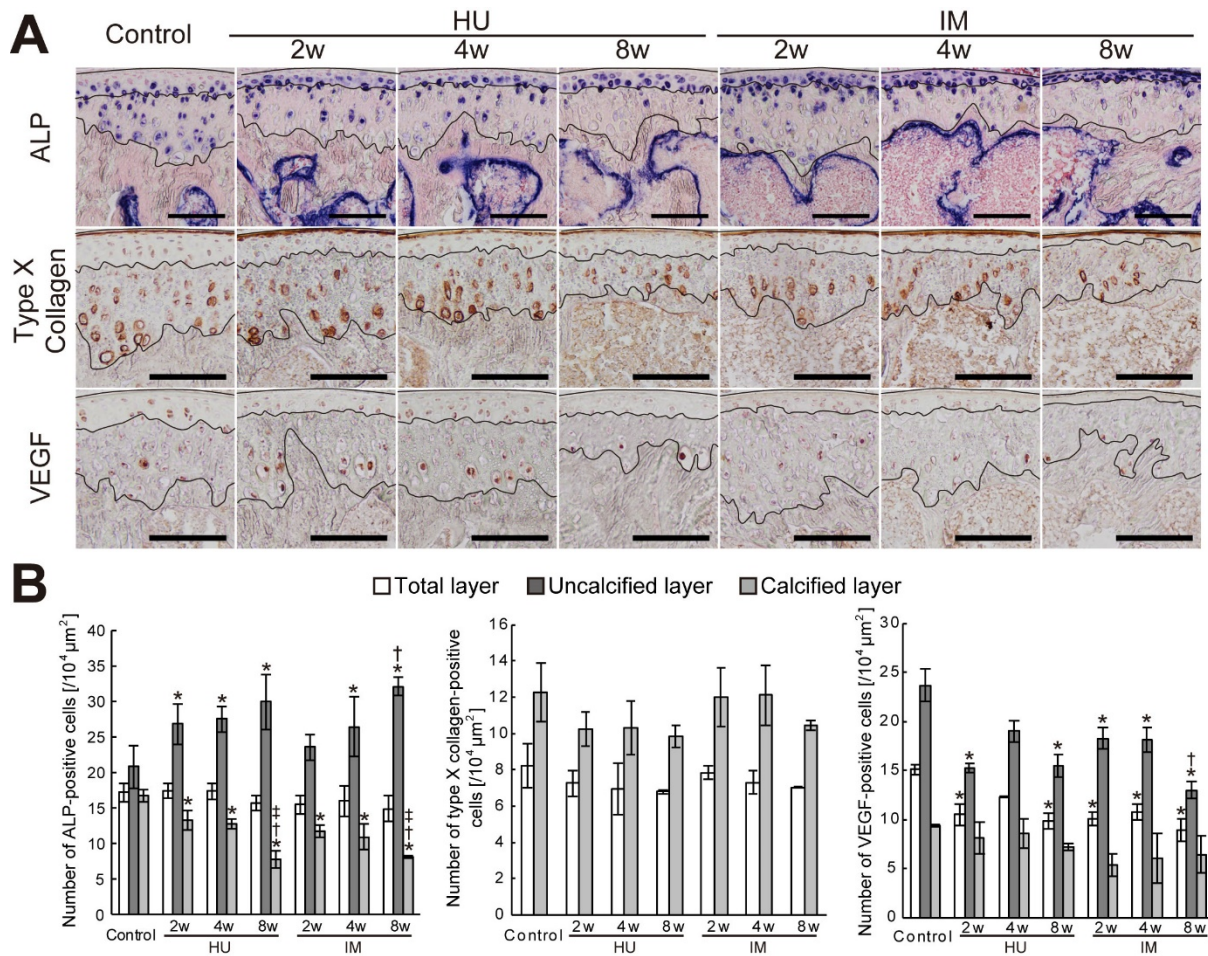
655 (upper row of aggrecan), 100 μm (lower row of aggrecan and upper row of ADAMTS5), 20

656 μm (lower row of ADAMTS5) (D) Staining intensity for aggrecan and the number of

657 ADAMTS5-positive cells. Mean values of the six regions. Results for each region are shown

658 in Supplementary Table 5 and 6. * Significant differences from the control group. †

659 Significant differences from the 2 weeks after the same intervention.



660

661

Fig. 4. Distributions of ALP activity and markers of chondrocyte hypertrophy. (A)

662

Progressive decrease in ALP-positive cells in calcified layer of articular cartilage were

663

observed in the HU and IM groups. Uncalcified cartilage in the IM group exhibited marked

664

increases in ALP activity. Immunostaining for type X collagen or VEGF was seen strongly at

665

calcified layer. Scale bars = 100 μm . (B) The numbers of ALP-, type X collagen-, and VEGF-

666

positive chondrocytes. Mean values of the six regions. Results for each region are shown in

667

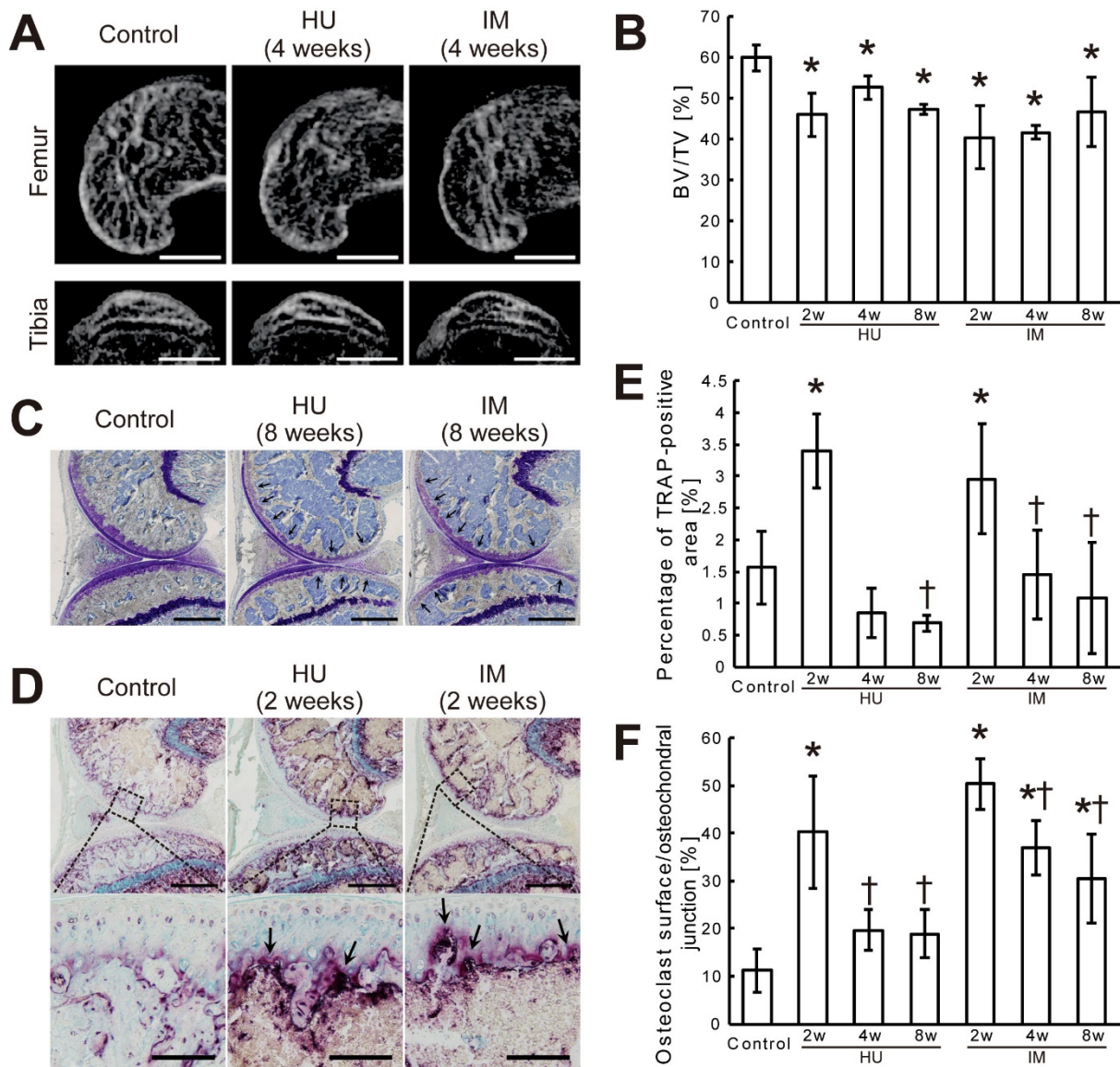
Supplementary Table 7, 8, and 9. * Significant differences from the control group. †

668

Significant differences from the 2 weeks after the same intervention. ‡ Significant differences

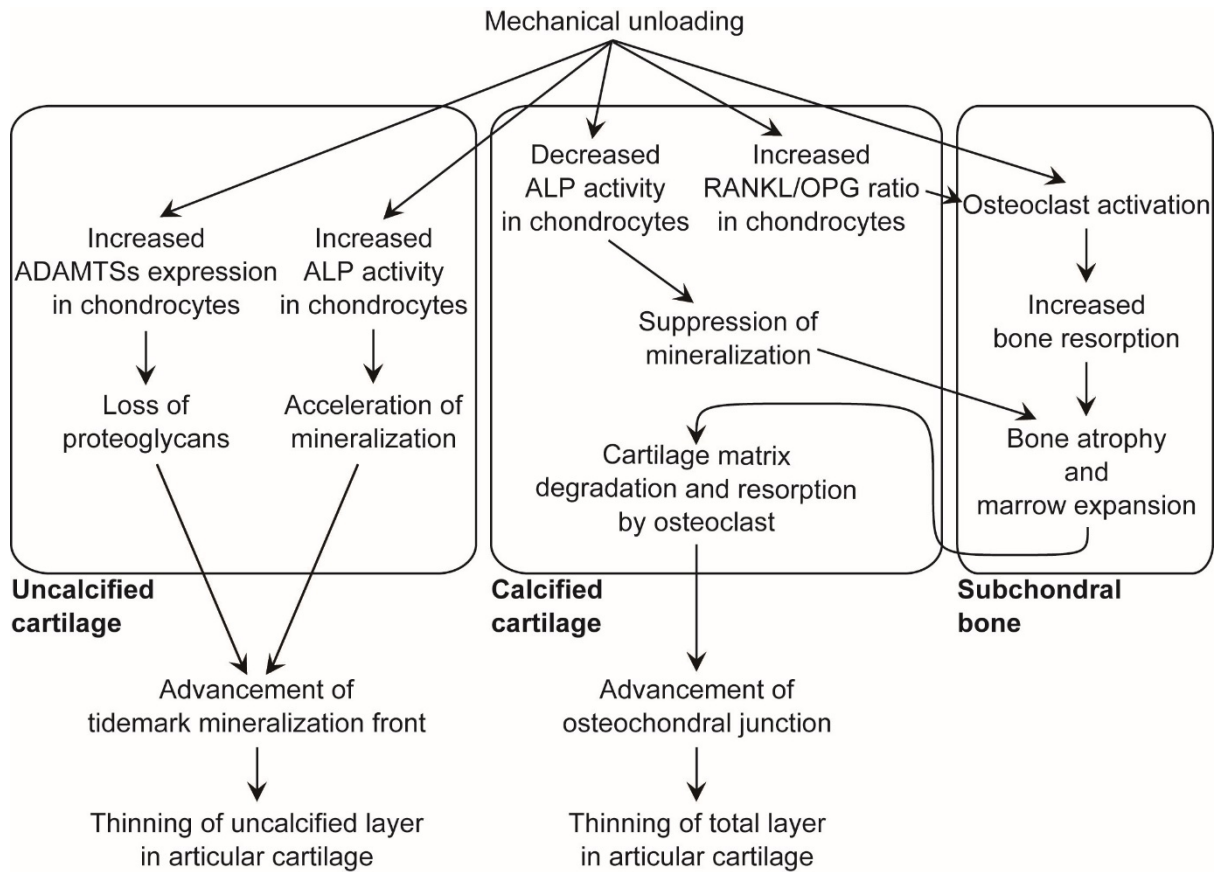
669

from the 4 weeks after the same intervention.



670
 671 **Fig. 5.** Bone structure and TRAP activity. (A) 3D images of distal femur and proximal tibia
 672 obtained by μ CT scanning. (B) Bone volume density (BV/TV) was quantified based on μ CT
 673 data. (C) Representative histological images of the whole knee joint stained with toluidine
 674 blue. Associated with loss of trabecular and subchondral bone, expanded bone marrow space
 675 reached the articular cartilage (arrows). Scale bars = 500 μ m. (D) Representative histological
 676 sections stained with TRAP/alcian blue. Scale bars = 500 μ m (upper row), 100 μ m (lower
 677 row). The HU and IM groups showed increased TRAP activity at entire epiphysis at 2 weeks,

678 and the activity invaded into calcified layer of articular cartilage (arrow). (E) Percentage of
679 TRAP-positive area at epiphyseal region. (F) Osteoclast surface reaching cartilaginous layer
680 per osteochondral junction. * Significant differences from the control group. † Significant
681 differences from the 2 weeks after the same intervention.



682

683

Fig. 6. Schema of unloading-induced articular cartilage thinning. Increased ALP activity with

684

concomitant loss of proteoglycans associated with increased aggrecanase expression at

685

uncalcified cartilage leads to tidemark advancement toward the articular surface, resulting in

686

thinning of uncalcified layer of articular cartilage. Subchondral osteoclast activation, which is

687

partly induced by increased RANKL/OPG ratio in articular chondrocytes, induces

688

subchondral bone atrophy. Decreased ALP activity in chondrocytes at calcified cartilage

689

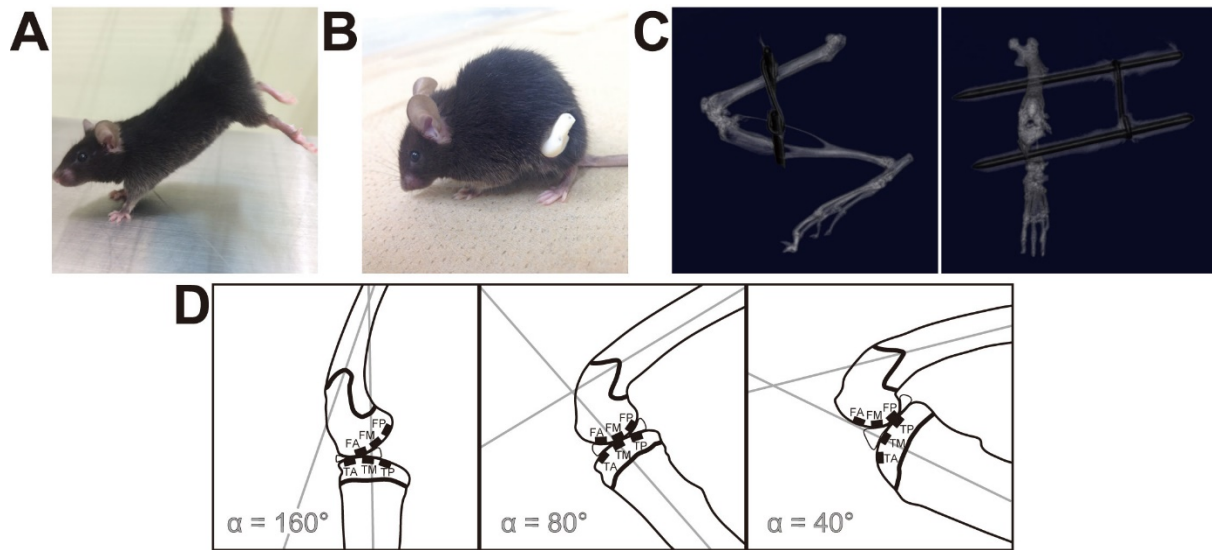
allows subchondral marrow space to invade articular cartilage. Advancement of

690

osteochondral junction through cartilage matrix degradation and resorption by osteoclast

691

results in thinning of total layer in articular cartilage.



692

693 **Supplementary Fig. 1.** Animal models and relative position of the regions for assessment.

694 (A) Tail suspended mice maintained their hindlimbs at extended position. (B) Mice treated

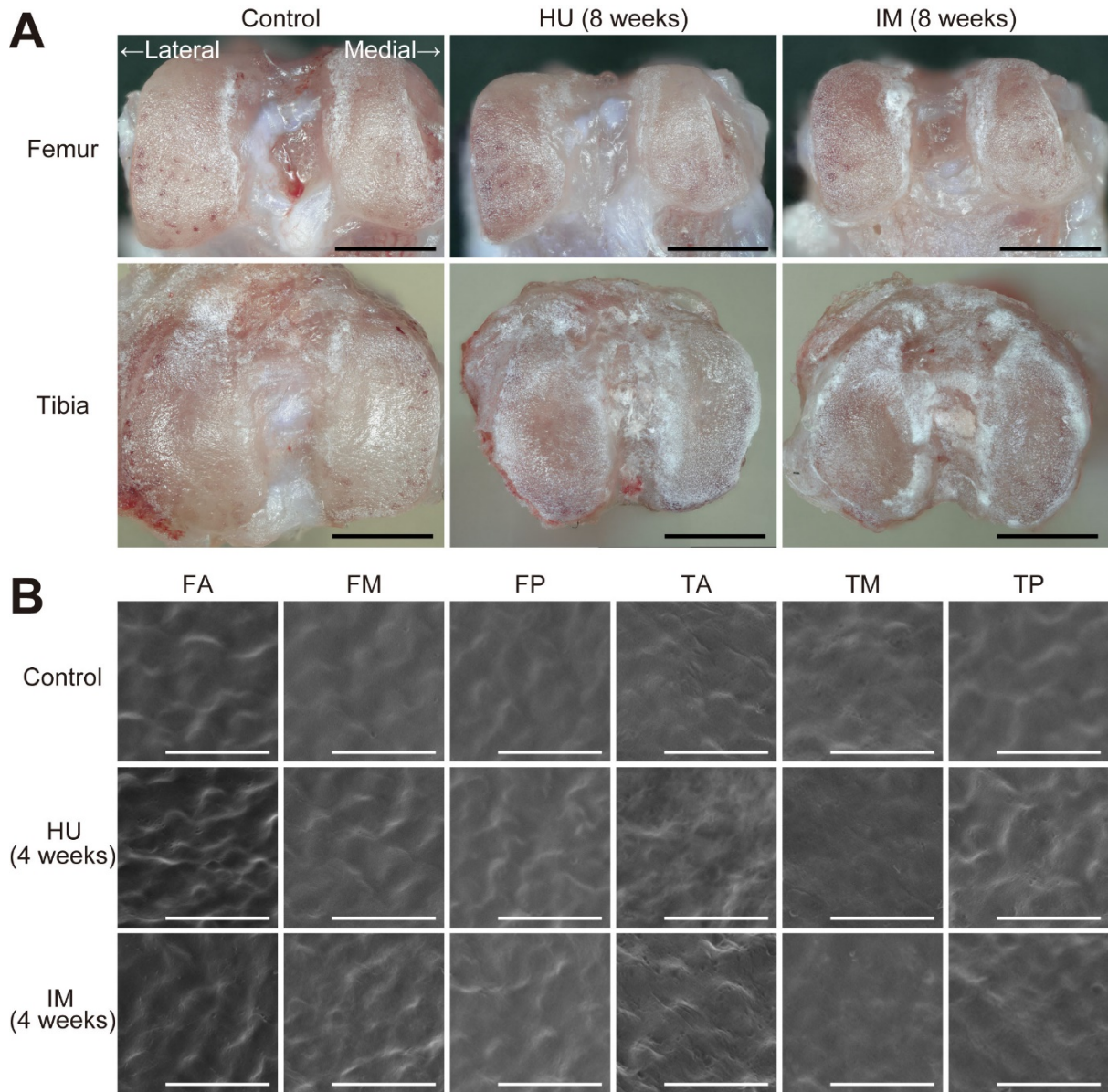
695 with surgical immobilization of the knee joints exhibited bilaterally symmetric standing and

696 ambulation. (C) Confirmation of joint fixation. μ CT scanning revealed that kirschner wires

697 penetrated through bones. (left) lateral view. (right) frontal view. (D) Positions of cartilage

698 regions when the knee joint angle (α) is 40° (maximal flexion; immobilized), 80° (typical

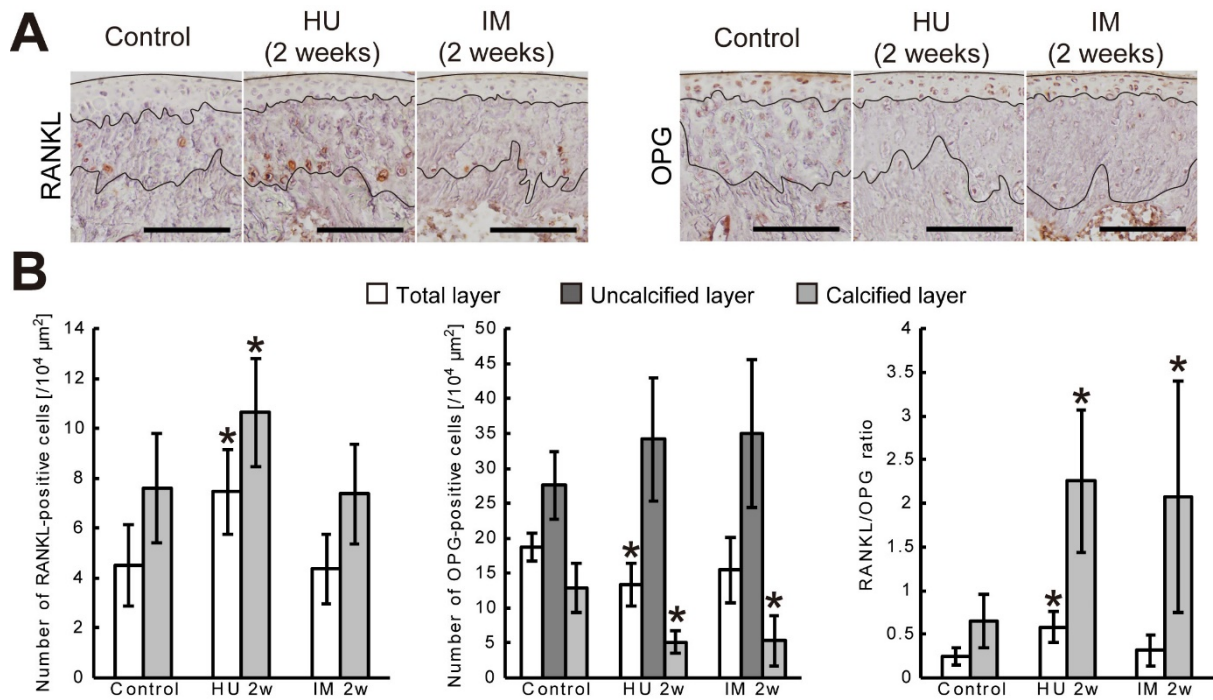
699 joint angle; control), 160° (maximal extension; hindlimb unloaded).



700

701 **Supplementary Fig. 2.** (A) Macroscopic (scale bars = 1 mm) and (B) Scanning Electron

702 Microscopic (SEM; scale bars = 50 μm) observations of articular surface of the knee joints.



703

704 **Supplementary Fig. 3.** Expressions of RANKL and OPG in articular chondrocytes. (A)

705 Representative immunohistochemical staining images. Scale bars = 100 μm . (B) Numbers of

706 RANKL- and OPG-positive chondrocytes were counted and RANKL/OPG ratio were

707 calculated. * Significant differences from the control group.

708 **Supplementary Table 1.** Cartilage thickness (μm) at each region after hindlimb unloading or joint immobilization.

Region	Layer	Control	Hindlimb Unloading			Joint Immobilization		
			2w	4w	8w	2w	4w	8w
FA	Total	128.1 \pm 9.2	126.5 \pm 19.5	112.5 \pm 9.9	94.7 \pm 7.2*†	119.1 \pm 11.0	102.2 \pm 5.9*	92.7 \pm 15.3*†
	Uncalcified	37.5 \pm 2.6	32.3 \pm 1.6*	29.2 \pm 0.3*	29.4 \pm 3.0*	31.8 \pm 4.0	28.9 \pm 3.4	27.1 \pm 8.6*
	Calcified	90.5 \pm 7.5	94.2 \pm 18.0	83.3 \pm 9.7	65.3 \pm 5.0*†	87.4 \pm 7.4	73.3 \pm 8.4*	65.5 \pm 8.8*†
FM	Total	121.2 \pm 5.0	122.9 \pm 18.4	115.4 \pm 13.4	94.6 \pm 7.0*†	104.4 \pm 14.1	97.7 \pm 7.8*	81.3 \pm 10.2*†
	Uncalcified	44.0 \pm 3.3	35.3 \pm 5.3*	33.5 \pm 4.2*	31.9 \pm 3.7*	35.7 \pm 6.8	31.9 \pm 2.1*	31.2 \pm 5.3*
	Calcified	77.3 \pm 5.4	87.6 \pm 13.9	81.8 \pm 10.7	62.7 \pm 10.2†	68.7 \pm 7.6	65.8 \pm 5.9	50.1 \pm 6.6*†‡
FP	Total	112.3 \pm 8.7	101.0 \pm 7.5	94.3 \pm 3.9*	84.7 \pm 3.2*†	98.9 \pm 10.3	91.5 \pm 5.4	84.3 \pm 18.3*
	Uncalcified	37.5 \pm 2.1	26.7 \pm 4.2*	30.5 \pm 2.1*	28.5 \pm 2.1*	35.4 \pm 0.4	35.3 \pm 2.1	31.5 \pm 1.5*†‡
	Calcified	74.8 \pm 7.0	74.3 \pm 4.4	63.9 \pm 4.8*	56.2 \pm 2.8*†	63.4 \pm 10.4	56.3 \pm 4.4	52.8 \pm 16.9*
TA	Total	93.5 \pm 4.1	113.7 \pm 9.9*	111.4 \pm 4.5*	96.9 \pm 8.8†‡	84.2 \pm 2.4	86.1 \pm 5.1	89.2 \pm 11.4
	Uncalcified	46.7 \pm 2.7	43.0 \pm 7.0	40.4 \pm 3.1	36.9 \pm 3.6*	36.2 \pm 1.4*	30.6 \pm 5.8*	19.4 \pm 4.1*†‡
	Calcified	46.9 \pm 5.0	70.7 \pm 4.5*	71.0 \pm 4.2*	59.9 \pm 12.3	48.0 \pm 1.6	55.5 \pm 3.3	69.7 \pm 8.4*†‡
TM	Total	127.7 \pm 6.7	140.3 \pm 5.3*	129.6 \pm 2.6†	119.7 \pm 2.2†	118.5 \pm 6.2	118.4 \pm 5.6	112.5 \pm 6.1*
	Uncalcified	85.2 \pm 7.1	83.6 \pm 5.2	74.8 \pm 2.4*	66.5 \pm 5.7*†	76.2 \pm 5.5	70.1 \pm 4.6*	58.4 \pm 5.5*
	Calcified	42.6 \pm 7.1	56.7 \pm 6.2*	54.7 \pm 1.6*	53.2 \pm 5.1	42.2 \pm 4.7	48.3 \pm 5.8	54.1 \pm 8.8
TP	Total	116.2 \pm 7.6	117.1 \pm 14.4	110.1 \pm 8.9	92.5 \pm 2.2*†	111.8 \pm 14.4	107.5 \pm 15.4	103.0 \pm 4.2
	Uncalcified	48.5 \pm 3.3	42.6 \pm 5.4	36.4 \pm 3.9*	34.0 \pm 1.7*†	43.2 \pm 2.6	43.3 \pm 6.7	46.8 \pm 4.1
	Calcified	67.7 \pm 7.8	74.5 \pm 13.9	73.7 \pm 5.0	58.5 \pm 3.3	68.7 \pm 15.2	64.2 \pm 16.8	56.2 \pm 3.2

709 * Significant differences from the control group.

710 † Significant differences from the 2 weeks after the same intervention.

711 ‡ Significant differences from the 4 weeks after the same intervention.

712 **Supplementary Table 2.** Chondrocyte density ($/10^4 \mu\text{m}^2$) at each region after hindlimb unloading or joint immobilization.

Region	Layer	Control	Hindlimb Unloading			Joint Immobilization		
			2w	4w	8w	2w	4w	8w
FA	Total	19.0 ± 4.3	14.1 ± 1.9	14.1 ± 1.2	14.3 ± 2.0	7.2 ± 2.3*	4.8 ± 1.4*	3.9 ± 2.0*
	Uncalcified	43.6 ± 16.2	36.1 ± 6.1	38.1 ± 7.3	35.4 ± 5.5	12.6 ± 4.4*	7.0 ± 5.1*	8.6 ± 6.5*
	Calcified	10.7 ± 1.4	7.5 ± 1.8*	5.9 ± 1.6*	5.3 ± 1.2*	5.5 ± 1.9*	3.8 ± 0.3*	2.6 ± 1.0*
FM	Total	16.4 ± 3.8	14.4 ± 1.6	14.1 ± 1.5	15.9 ± 3.6	7.5 ± 3.9*	6.1 ± 1.7*	6.2 ± 2.9*
	Uncalcified	34.9 ± 10.3	37.5 ± 3.2	35.1 ± 8.9	36.8 ± 7.2	13.7 ± 6.0*	15.3 ± 2.9*	11.1 ± 3.8*
	Calcified	7.1 ± 1.4	5.6 ± 1.5	6.6 ± 1.3	6.1 ± 2.3	4.3 ± 1.6	2.0 ± 1.5*	3.5 ± 2.5*
FP	Total	13.7 ± 4.6	13.5 ± 1.6	15.9 ± 2.6	14.0 ± 1.4	9.1 ± 1.5	10.5 ± 3.4	7.0 ± 4.4
	Uncalcified	26.4 ± 11.2	36.4 ± 8.6	39.8 ± 8.9	31.0 ± 10.3	15.3 ± 3.8	19.7 ± 7.5	12.2 ± 8.2
	Calcified	7.1 ± 2.8	5.9 ± 2.3	6.9 ± 3.0	6.2 ± 1.9	4.5 ± 1.5	5.7 ± 2.0	4.1 ± 1.5
TA	Total	15.7 ± 4.3	15.7 ± 3.5	16.3 ± 2.2	15.6 ± 2.2	4.7 ± 3.8*	6.8 ± 3.3*	8.1 ± 3.8*
	Uncalcified	28.6 ± 8.3	35.5 ± 3.9	36.0 ± 8.9	33.7 ± 3.4	7.2 ± 8.3*	10.4 ± 8.0	21.9 ± 18.2
	Calcified	3.3 ± 0.6	4.3 ± 2.1	5.2 ± 1.5	4.8 ± 1.2	3.2 ± 1.1	4.7 ± 3.6	3.1 ± 1.1
TM	Total	15.2 ± 4.8	13.2 ± 1.3	15.5 ± 2.0	13.6 ± 2.7	8.9 ± 2.9	11.7 ± 2.0	7.9 ± 3.1*
	Uncalcified	20.7 ± 7.4	19.4 ± 0.7	21.5 ± 1.5	21.1 ± 3.1	12.7 ± 5.3	17.8 ± 4.4	11.6 ± 5.4
	Calcified	4.9 ± 0.9	3.7 ± 2.1	7.5 ± 3.3	5.3 ± 3.9	2.6 ± 1.7	2.9 ± 1.7	3.8 ± 1.3
TP	Total	13.3 ± 4.3	15.2 ± 3.3	13.6 ± 0.8	14.1 ± 0.3	10.0 ± 4.5	13.3 ± 3.6	10.1 ± 3.6
	Uncalcified	29.6 ± 13.0	35.6 ± 7.8	35.1 ± 5.4	34.5 ± 2.8	18.8 ± 9.2	26.5 ± 6.4	16.1 ± 5.0
	Calcified	5.5 ± 0.9	5.4 ± 2.1	4.1 ± 1.0	4.5 ± 1.1	4.7 ± 0.8	5.1 ± 2.1	5.8 ± 2.1

713 * Significant differences from the control group.

714 † Significant differences from the 2 weeks after the same intervention.

715 ‡ Significant differences from the 4 weeks after the same intervention.

716 **Supplementary Table 3.** Staining intensity for type II collagen at each region after hindlimb unloading or joint immobilization.

Region	Layer	Control	Hindlimb Unloading			Joint Immobilization		
			2w	4w	8w	2w	4w	8w
FA	Total	135.7 ± 9.9	140.1 ± 5.2	131.2 ± 7.0	134.2 ± 7.0	132.2 ± 7.6	134.7 ± 5.1	140.3 ± 5.6
	Uncalcified	143.1 ± 13.8	152.9 ± 8.9	146.8 ± 4.5	142.8 ± 6.2	143.9 ± 9.6	146.9 ± 7.3	150.1 ± 5.0
	Calcified	133.5 ± 9.1	136.1 ± 4.5	126.7 ± 7.8	130.5 ± 8.2	128.9 ± 8.6	129.6 ± 8.2	135.7 ± 7.8
FM	Total	124.4 ± 12.6	126.5 ± 1.7	115.9 ± 3.9	117.9 ± 3.2	121.6 ± 13.3	120.2 ± 10.2	132.0 ± 6.2
	Uncalcified	125.6 ± 14.2	124.9 ± 4.9	115.3 ± 4.7	112.2 ± 6.9	120.7 ± 16.3	120.7 ± 6.3	136.9 ± 10.7
	Calcified	124.2 ± 13.5	127.3 ± 3.0	116.2 ± 3.8	120.3 ± 1.2	123.8 ± 13.7	120.7 ± 12.0	131.2 ± 7.1
FP	Total	125.3 ± 13.8	134.6 ± 1.7	119.8 ± 6.1	116.6 ± 7.2	129.9 ± 10.9	120.4 ± 13.4	141.8 ± 10.9
	Uncalcified	124.4 ± 17.5	122.0 ± 3.2	104.1 ± 4.1	102.1 ± 4.5*	120.9 ± 10.1	114.1 ± 9.0	136.3 ± 12.2
	Calcified	126.9 ± 12.9	140.1 ± 4.4	126.6 ± 6.9	124.4 ± 11.3	138.1 ± 13.1	127.1 ± 16.5	148.0 ± 12.1
TA	Total	115.4 ± 13.6	111.9 ± 6.4	122.0 ± 5.6	132.4 ± 6.1	120.6 ± 5.9	122.8 ± 7.5	110.7 ± 7.7
	Uncalcified	106.9 ± 16.7	104.3 ± 8.3	112.3 ± 2.0	122.0 ± 7.6	112.5 ± 6.3	113.4 ± 9.0	106.8 ± 8.8
	Calcified	123.4 ± 11.7	114.2 ± 6.2	124.1 ± 8.5	137.1 ± 4.9†	121.3 ± 9.4	130.3 ± 6.5	112.8 ± 7.5
TM	Total	129.6 ± 14.4	127.4 ± 5.5	123.5 ± 4.6	113.5 ± 2.1	126.5 ± 8.0	125.6 ± 7.4	137.7 ± 9.4
	Uncalcified	133.9 ± 19.0	130.8 ± 7.4	125.6 ± 4.1	115.6 ± 5.7	130.7 ± 8.9	129.5 ± 4.7	140.4 ± 7.2
	Calcified	126.1 ± 10.3	124.3 ± 6.3	120.8 ± 4.7	111.6 ± 2.2	118.9 ± 9.3	121.1 ± 10.7	134.5 ± 14.3
TP	Total	126.7 ± 14.4	123.7 ± 2.4	119.6 ± 5.8	117.5 ± 4.6	127.2 ± 13.2	127.4 ± 10.4	136.8 ± 10.2
	Uncalcified	137.6 ± 18.4	130.2 ± 0.7	126.0 ± 5.7	125.0 ± 9.7	138.1 ± 12.9	139.8 ± 2.7	144.2 ± 12.0
	Calcified	122.0 ± 13.2	122.4 ± 1.1	116.7 ± 6.2	113.3 ± 3.9	123.3 ± 13.6	126.2 ± 16.2	132.4 ± 13.5

717 * Significant differences from the control group.

718 † Significant differences from the 2 weeks after the same intervention.

719 **Supplementary Table 4.** Number of MMP13-positive cells ($/10^4 \mu\text{m}^2$) at each region after hindlimb unloading or joint immobilization.

Region	Layer	Control	Hindlimb Unloading			Joint Immobilization		
			2w	4w	8w	2w	4w	8w
FA	Total	3.6 ± 1.4	3.3 ± 1.0	4.8 ± 0.7	2.8 ± 1.1	2.5 ± 1.0	2.9 ± 0.6	1.8 ± 0.8
	Calcified	5.0 ± 2.0	4.4 ± 1.2	6.5 ± 1.1	3.9 ± 1.3	3.3 ± 1.5	4.1 ± 0.3	2.4 ± 1.0
FM	Total	1.6 ± 1.3	3.0 ± 1.0	4.1 ± 1.9	$4.2 \pm 0.8^*$	1.9 ± 1.0	3.5 ± 0.9	1.9 ± 1.0
	Calcified	2.6 ± 2.1	4.2 ± 1.1	5.5 ± 2.5	$6.2 \pm 0.9^*$	3.0 ± 1.7	5.1 ± 1.4	3.2 ± 1.5
FP	Total	3.6 ± 1.0	3.6 ± 1.1	3.9 ± 0.9	4.1 ± 2.3	3.2 ± 2.3	4.5 ± 1.3	2.7 ± 0.6
	Calcified	5.3 ± 1.7	5.1 ± 1.7	6.0 ± 1.6	6.0 ± 3.1	5.4 ± 3.7	7.2 ± 1.8	4.2 ± 0.7
TA	Total	2.5 ± 1.2	2.0 ± 1.0	3.2 ± 1.6	3.2 ± 0.6	2.6 ± 0.9	1.9 ± 0.8	1.5 ± 0.8
	Calcified	5.3 ± 2.6	3.1 ± 1.4	5.1 ± 2.5	5.6 ± 0.8	4.9 ± 1.4	3.4 ± 0.9	2.4 ± 1.5
TM	Total	2.9 ± 0.8	4.0 ± 2.6	4.3 ± 1.1	5.5 ± 3.2	1.9 ± 0.6	2.5 ± 1.1	2.9 ± 1.2
	Calcified	8.9 ± 3.4	11.6 ± 8.5	10.7 ± 1.8	12.5 ± 7.1	5.6 ± 1.5	6.3 ± 2.7	7.6 ± 3.8
TP	Total	4.8 ± 2.5	3.0 ± 1.0	4.1 ± 1.5	4.0 ± 3.1	3.1 ± 0.8	4.7 ± 2.6	4.4 ± 2.1
	Calcified	7.6 ± 3.8	4.3 ± 1.0	5.6 ± 2.2	5.7 ± 4.2	4.6 ± 1.0	7.6 ± 4.5	7.1 ± 2.9

720 * Significant differences from the control group.

721 **Supplementary Table 5.** Staining intensity for aggrecan at each region after hindlimb unloading or joint immobilization.

Region	Layer	Control	Hindlimb Unloading			Joint Immobilization		
			2w	4w	8w	2w	4w	8w
FA	Total	102.7 ± 4.3	95.7 ± 4.4	106.3 ± 4.1†	109.3 ± 4.5†	91.5 ± 4.5*	97.0 ± 3.7	95.7 ± 5.9
	Uncalcified	104.2 ± 6.4	91.1 ± 6.6*	102.5 ± 5.9	103.4 ± 5.1	84.3 ± 2.8*	94.8 ± 4.7	93.7 ± 6.9
	Calcified	102.1 ± 3.5	97.8 ± 5.4	106.4 ± 5.0	108.4 ± 6.1	93.2 ± 5.4*	96.9 ± 3.9	94.9 ± 5.9
FM	Total	96.8 ± 3.2	91.5 ± 3.1	98.4 ± 4.6	101.8 ± 2.1†	86.1 ± 2.3*	92.0 ± 0.3	95.5 ± 5.8†
	Uncalcified	94.9 ± 3.6	82.7 ± 3.5*	88.8 ± 5.4	92.2 ± 2.5†	77.8 ± 3.9*	88.3 ± 1.6†	96.4 ± 8.7†
	Calcified	98.9 ± 3.2	94.4 ± 3.2	101.3 ± 5.1	105.6 ± 2.2*†	90.6 ± 2.7*	94.7 ± 2.2	95.1 ± 5.3
FP	Total	94.8 ± 4.2	94.7 ± 4.0	100.3 ± 0.5	101.3 ± 1.8*	93.0 ± 2.9	103.0 ± 3.2*†	100.9 ± 3.6†
	Uncalcified	89.5 ± 4.0	80.5 ± 4.0*†	84.1 ± 3.6	81.8 ± 5.4	85.9 ± 6.0	109.1 ± 9.6*†	103.7 ± 10.3*†
	Calcified	99.5 ± 4.2	98.9 ± 5.0	104.7 ± 1.1	106.5 ± 2.3*†	98.4 ± 1.5	100.2 ± 2.9	100.1 ± 4.3
TA	Total	99.9 ± 6.2	100.0 ± 5.7	101.5 ± 6.3	100.3 ± 5.2	87.1 ± 4.4*	93.6 ± 2.1	94.1 ± 5.1
	Uncalcified	104.4 ± 7.0	97.9 ± 10.8	103.6 ± 5.8	101.3 ± 2.8	82.4 ± 5.9*	96.7 ± 2.7†	102.7 ± 4.6†
	Calcified	98.3 ± 8.5	100.3 ± 5.9	102.1 ± 8.3	100.3 ± 5.9	88.4 ± 4.0	92.9 ± 4.2	91.3 ± 4.6
TM	Total	100.2 ± 5.6	93.4 ± 4.8	97.8 ± 5.0	102.1 ± 4.0	91.3 ± 3.6*	96.6 ± 2.4	94.5 ± 1.4
	Uncalcified	103.6 ± 6.8	92.8 ± 8.7	98.2 ± 6.9	104.1 ± 2.2	90.6 ± 5.7*	100.0 ± 3.5	94.8 ± 2.5
	Calcified	100.1 ± 4.4	96.7 ± 3.2	98.8 ± 6.6	102.4 ± 6.4	95.4 ± 4.5	95.8 ± 4.4	95.6 ± 2.4
TP	Total	101.2 ± 9.8	93.3 ± 2.6*	99.4 ± 1.6	97.1 ± 5.0	96.7 ± 5.4	106.9 ± 7.1	104.2 ± 9.7
	Uncalcified	109.0 ± 14.0	86.6 ± 1.5	92.8 ± 6.2	98.3 ± 6.9	96.5 ± 11.8	120.5 ± 10.4	109.2 ± 13.9
	Calcified	100.1 ± 7.7	93.1 ± 1.9	100.1 ± 3.7	96.2 ± 4.7	96.8 ± 5.7	107.3 ± 6.7	104.4 ± 9.4

722 * Significant differences from the control group.

723 † Significant differences from the 2 weeks after the same intervention.

724 **Supplementary Table 6.** Number of ADAMTS5-positive cells ($/10^4 \mu\text{m}^2$) at each region after hindlimb unloading or joint immobilization.

Region	Layer	Control	Hindlimb Unloading			Joint Immobilization		
			2w	4w	8w	2w	4w	8w
FA	Total	16.2 ± 4.0	13.9 ± 1.1	15.9 ± 1.6	18.5 ± 5.0	19.9 ± 1.7	22.4 ± 3.4	17.1 ± 7.4
	Uncalcified	31.4 ± 5.0	33.8 ± 6.5	41.1 ± 1.9	39.0 ± 7.2	57.8 ± 4.3*	52.6 ± 12.9	38.7 ± 23
	Calcified	9.7 ± 2.6	7.8 ± 1.6	7.0 ± 2.2	8.8 ± 3.9	6.0 ± 1.9	10.3 ± 3.2	9.8 ± 6.1
FM	Total	15.5 ± 2.3	16.2 ± 4.6	14.4 ± 2.3	15.6 ± 3.0	19.2 ± 3.8	19.7 ± 3.3	18.5 ± 4.9
	Uncalcified	26.9 ± 4.5	35.6 ± 13.5	32.2 ± 5.4	31.6 ± 9.1	43.8 ± 13.8*	36.7 ± 4.8	34.3 ± 6.0
	Calcified	8.8 ± 2.1	8.1 ± 2.0	7.3 ± 1.6	7.5 ± 1.4	7.8 ± 2.0	8.9 ± 2.1	7.7 ± 4.2
FP	Total	5.9 ± 2.4	21.0 ± 7.2*	18.6 ± 4.4*	20.8 ± 4.1*	12.0 ± 7.0	6.9 ± 2.3	8.1 ± 4.3
	Uncalcified	10.3 ± 5.0	40.6 ± 8.0*	34.3 ± 6.1*	43.8 ± 7.4*	20.8 ± 10.4	11.8 ± 7.6	12.1 ± 13.6
	Calcified	3.4 ± 1.6	9.3 ± 6.1	8.2 ± 3.7	8.9 ± 2.6	5.2 ± 2.6	4.1 ± 1.5	4.7 ± 3.4
TA	Total	16.1 ± 4.8	12.6 ± 2.5	16.7 ± 2.4	14.6 ± 1.9	17.8 ± 2.9	22.7 ± 5.4	18.7 ± 3.8
	Uncalcified	23.6 ± 7.1	23.4 ± 7.0	31.8 ± 4.7	26.1 ± 5.3	31.1 ± 3.9	39.3 ± 12.3	45.9 ± 17.4*
	Calcified	5.4 ± 3.7	6.0 ± 1.3	5.6 ± 2.6	8.3 ± 3.1	5.1 ± 4.9	7.8 ± 1.3	6.8 ± 1.3
TM	Total	13.7 ± 2.0	13.2 ± 0.5	18.6 ± 2.8*†	16.3 ± 2.3	19.4 ± 3.6*	14.6 ± 3.8	14.7 ± 1.9
	Uncalcified	17.1 ± 1.5	18.3 ± 2.3	26.2 ± 5.3*†	24.2 ± 3.4*	23.2 ± 3.6*	16.7 ± 2.9	21.4 ± 4.7
	Calcified	7.2 ± 3.7	5.1 ± 1.2	7.2 ± 3.2	5.5 ± 2.4	12.5 ± 4.8	11.3 ± 7.8	5.8 ± 2.2
TP	Total	11.5 ± 2.6	17.9 ± 4.4	13.9 ± 3.5	20.4 ± 8.7	14.6 ± 5.3	11.6 ± 4.9	8.1 ± 4.1
	Uncalcified	19.3 ± 5.2	44.0 ± 13.7*	33.4 ± 11.8	47.9 ± 22.9	25.7 ± 9.5	16.3 ± 12.5	10.2 ± 10.6
	Calcified	5.9 ± 1.8	4.8 ± 1.7	5.1 ± 1.0	6.1 ± 2.2	7.5 ± 3.9	8.1 ± 2.6	6.5 ± 1.2

725 * Significant differences from the control group.

726 † Significant differences from the 2 weeks after the same intervention.

727 **Supplementary Table 7.** Number of ALP-positive cells ($/10^4 \mu\text{m}^2$) at each region after hindlimb unloading or joint immobilization.

Region	Layer	Control	Hindlimb Unloading			Joint Immobilization		
			2w	4w	8w	2w	4w	8w
FA	Total	21.2 ± 3.2	21.2 ± 2.7	21.1 ± 3.9	19.4 ± 1.6	20.5 ± 1.2	22.1 ± 5.0	23.3 ± 4.7
	Uncalcified	38.6 ± 11.6	37.3 ± 6.4	35.6 ± 6.2	41.1 ± 5.6	44.5 ± 4.4	47.7 ± 7.6	75.4 ± 16.6*†‡
	Calcified	15.6 ± 2.0	15.1 ± 3.9	14.4 ± 3.4	7.5 ± 3.3*†‡	12.9 ± 2.0	12.2 ± 4.7	10.8 ± 4.2
FM	Total	20.2 ± 4.2	18.4 ± 1.4	17.3 ± 2.8	15.6 ± 3.8	17.6 ± 3.6	20.9 ± 3.4	18.2 ± 2.0*
	Uncalcified	24.9 ± 4.3	28.6 ± 3.0	34.1 ± 7.1*	33.2 ± 3.9	29.2 ± 7.5	36.8 ± 7.5	38.6 ± 8.2
	Calcified	17.7 ± 4.4	14.0 ± 2.5	11.5 ± 2.1	7.0 ± 5.0*	11.9 ± 3.4	12.5 ± 3.1	7.5 ± 1.5*
FP	Total	19.1 ± 2.8	16.0 ± 2.5	18.0 ± 2.5	15.9 ± 1.6	14.9 ± 2.5	12.2 ± 2.5*	10.0 ± 5.0*
	Uncalcified	20.6 ± 5.5	30.3 ± 7.4	30.6 ± 4.0	30.1 ± 5.7	18.5 ± 3.8	18.5 ± 6.0	18.9 ± 8.9
	Calcified	18.3 ± 1.7	10.7 ± 1.9*	11.7 ± 2.3*	8.9 ± 3.1*	12.2 ± 2.4*	7.9 ± 1.9*	4.9 ± 2.6*†
TA	Total	14.8 ± 2.6	17.8 ± 2.6	15.8 ± 1.1	17.9 ± 7.8	16.3 ± 1.0	21.8 ± 3.8*	20.4 ± 2.4*
	Uncalcified	14.0 ± 1.7	27.2 ± 7.6	22.5 ± 2.4	37.1 ± 18.9*	23.2 ± 2.9	37.4 ± 13.7*†	38.2 ± 3.7*†
	Calcified	16.2 ± 5.7	11.9 ± 2.3	10.9 ± 2.0	7.5 ± 2.9*	10.5 ± 2.6	12.7 ± 1.7	11.6 ± 2.6
TM	Total	10.7 ± 1.6	12.4 ± 1.8	13.5 ± 1.8	10.8 ± 1.7	10.5 ± 2.6	11.6 ± 1.3	11.4 ± 1.1
	Uncalcified	7.1 ± 1.4	11.4 ± 1.2*	12.7 ± 1.6*	11.9 ± 1.2*	9.9 ± 2.5	11.1 ± 3.4	13.0 ± 5.0*
	Calcified	17.4 ± 3.0	14.0 ± 3.6	14.5 ± 3.8	9.3 ± 4.6*	11.8 ± 3.3	13.0 ± 3.6	10.2 ± 2.9*
TP	Total	17.5 ± 1.9	18.9 ± 2.5	18.8 ± 2.6	14.5 ± 0.7*†	13.0 ± 2.8*	7.4 ± 2.5*†	6.1 ± 0.9*†
	Uncalcified	19.6 ± 6.2	26.1 ± 1.7	29.6 ± 9.5	26.0 ± 4.5	16.3 ± 3.7	7.0 ± 2.8*	8.7 ± 2.9*
	Calcified	15.3 ± 2.6	14.2 ± 3.2	13.5 ± 1.6	6.6 ± 2.9*†‡	11.0 ± 3.6	7.7 ± 2.6*	4.2 ± 1.5*†

728 * Significant differences from the control group.

729 † Significant differences from the 2 weeks after the same intervention.

730 ‡ Significant differences from the 4 weeks after the same intervention.

731 **Supplementary Table 8.** Number of type X collagen-positive cells ($/10^4 \mu\text{m}^2$) at each region after hindlimb unloading or joint immobilization.

Region	Layer	Control	Hindlimb Unloading			Joint Immobilization		
			2w	4w	8w	2w	4w	8w
FA	Total	10.4 ± 1.1	9.9 ± 1.5	9.7 ± 1.4	9.1 ± 1.7	9.5 ± 3.9	9.1 ± 0.4	12.5 ± 1.1
	Calcified	13.3 ± 0.5	12.2 ± 1.6	12.9 ± 1.9	12.4 ± 2.4	12.3 ± 4.7	12.6 ± 1.7	14.5 ± 0.9
FM	Total	7.3 ± 0.3	6.3 ± 1.3	8.6 ± 4.0	8.6 ± 0.5	8.0 ± 1.3	9.3 ± 1.7	6.1 ± 0.4
	Calcified	10.2 ± 0.4	8.9 ± 0.4	11.9 ± 5.6	11.9 ± 2.1	11.1 ± 1.0	14.9 ± 0.7*†	8.9 ± 0.5‡
FP	Total	10.0 ± 4.2	7.1 ± 2.0	6.6 ± 2.1	8.1 ± 2.0	9.3 ± 1.4	8.4 ± 1.9	7.5 ± 1.7
	Calcified	14.9 ± 6.7	9.4 ± 2.9	8.5 ± 2.4	10.9 ± 1.5	13.9 ± 1.3	13.2 ± 3.5	12.7 ± 5.1
TA	Total	6.9 ± 1.2	7.4 ± 2.5	7.4 ± 1.0	4.6 ± 1.5	6.9 ± 4.1	4.7 ± 0.9	4.2 ± 0.7
	Calcified	12.4 ± 0.4	11.4 ± 5.2	11.3 ± 2.8	7.3 ± 1.7	11.1 ± 7.3	9.3 ± 0.4	6.8 ± 1.9
TM	Total	3.8 ± 1.6	5.0 ± 1.0	4.3 ± 0.4	3.6 ± 0.6	5.5 ± 3.1	4.5 ± 0.9	4.9 ± 0.3
	Calcified	9.2 ± 4.2	10.0 ± 1.4	10.2 ± 0.8	7.7 ± 0.3	11.1 ± 6.6	10.5 ± 0.0	9.0 ± 1.7
TP	Total	9.6 ± 1.3	7.7 ± 0.3	5.2 ± 1.6	6.4 ± 1.9	8.0 ± 1.1	7.7 ± 2.9	7.1 ± 0.3
	Calcified	13.8 ± 0.2	9.6 ± 0.2	7.3 ± 1.2*	8.8 ± 2.0*	12.6 ± 0.9	12.3 ± 5.7	10.7 ± 0.6

732 * Significant differences from the control group.

733 † Significant differences from the 2 weeks after the same intervention.

734 ‡ Significant differences from the 4 weeks after the same intervention.

735 **Supplementary Table 9.** Number of VEGF-positive cells ($/10^4 \mu\text{m}^2$) at each region after hindlimb unloading or joint immobilization.

Region	Layer	Control	Hindlimb Unloading			Joint Immobilization		
			2w	4w	8w	2w	4w	8w
FA	Total	16.8 ± 0.4	12.1 ± 2.0	12.5 ± 1.0	10.1 ± 3.7	8.6 ± 2.3	6.3 ± 1.7	8.4 ± 5.2
	Uncalcified	30.6 ± 9.5	19.7 ± 1.7	24.0 ± 0.5	15.5 ± 10.9	22.9 ± 7.0	13.3 ± 2.6	14.0 ± 19.8
	Calcified	12.0 ± 2.4	10.0 ± 2.2	8.7 ± 1.6	7.9 ± 0.7	4.8 ± 2.3	4.5 ± 1.2	6.3 ± 1.6
FM	Total	12.0 ± 2.3	7.9 ± 0.8	11.7 ± 1.1	10.1 ± 0.7	6.1 ± 1.1	7.7 ± 1.3	13.6 ± 2.1†
	Uncalcified	18.9 ± 0.5	10.1 ± 2.0	19.3 ± 7.1	17.0 ± 2.4	12.8 ± 0.1	16.4 ± 3.3	25.4 ± 3.2†
	Calcified	8.4 ± 3.3	7.2 ± 1.5	8.7 ± 1.5	7.6 ± 0.4	3.2 ± 0.8	3.0 ± 1.4	6.4 ± 5.1
FP	Total	15.5 ± 1.4	11.2 ± 0.2	8.0 ± 0.5*	9.4 ± 1.9*	11.7 ± 3.1	9.4 ± 0.2	6.9 ± 1.7*
	Uncalcified	25.4 ± 1.1	15.5 ± 4.3	9.4 ± 0.0	17.0 ± 6.9	17.8 ± 5.1	11.9 ± 8.0	2.7 ± 1.1*
	Calcified	9.1 ± 1.3	9.4 ± 1.4	7.3 ± 0.8	6.2 ± 0.4	8.0 ± 2.3	8.0 ± 4.1	8.8 ± 2.5
TA	Total	15.1 ± 1.4	11.2 ± 1.2	15.3 ± 5.2	7.8 ± 0.8	7.7 ± 1.6	18.9 ± 1.3	8.1 ± 3.7
	Uncalcified	24.5 ± 1.8	19.5 ± 8.8	22.1 ± 7.6	9.8 ± 1.9	14.4 ± 2.4	31.9 ± 3.9†	19.2 ± 14.6‡
	Calcified	8.8 ± 0.6	7.4 ± 1.7	11.8 ± 4.6	6.4 ± 2.7	3.3 ± 1.3	6.9 ± 4.2	2.5 ± 1.1
TM	Total	14.7 ± 1.0	10.1 ± 1.3	13.5 ± 1.6	11.4 ± 4.5	12.9 ± 2.4	11.7 ± 1.4	9.6 ± 3.4
	Uncalcified	16.9 ± 1.7	12.7 ± 0.5	17.1 ± 4.3	14.1 ± 8.3	19.1 ± 2.6	13.3 ± 1.2	14.6 ± 5.3
	Calcified	10.9 ± 0.2	5.9 ± 4.2	6.6 ± 3.8	8.3 ± 0.2	4.3 ± 0.1	8.6 ± 6.2	4.0 ± 1.3
TP	Total	16.5 ± 1.7	10.3 ± 1.3	12.6 ± 2.7	10.3 ± 0.6	13.5 ± 1.5	10.6 ± 0.8	7.1 ± 1.8*†
	Uncalcified	25.9 ± 1.2	14.1 ± 0.9*	22.2 ± 2.1†	19.6 ± 2.2	22.7 ± 5.3	21.8 ± 0.4	2.2 ± 3.2*†‡
	Calcified	7.0 ± 1.1	8.6 ± 2.1	8.3 ± 1.8	7.0 ± 0.1	8.8 ± 0.4	5.5 ± 1.8	10.8 ± 0.4‡

736 * Significant differences from the control group.

737 † Significant differences from the 2 weeks after the same intervention.

738 ‡ Significant differences from the 4 weeks after the same intervention.